

segment, worsening of chest pain), and (4) the association of SNPs of ANP-related genes with response to ANP treatment. SNPs of genes that may influence the occurrence of AMI are compared between patients enrolled in J-WIND-ANP and normal subjects. In addition, the optimal combination of therapeutic drugs to treat patients post-MI will be retrospectively surveyed by data mining. Clinical characteristics and medication during the follow-up period must be reported to the J-WIND-ANP Data and Safety Committee at 3, 6, 12 and 24 months after registration.

Safety

The Safety and Data Monitoring Committee, comprising 3 physicians and a statistician not involved in the conduct of the trial, monitors all adverse events. Furthermore, research nurses visit the participating hospitals to check that the registration, administration of drugs and data collection are correctly performed according to the protocol. Interim analyses of study data will be performed when approximately 20%, 40%, and 60% of the expected number of patients have been enrolled. The committee members do not communicate any results to the Steering Committee, unless discontinuation of the study is recommended.

Sample Size

A previous single center study demonstrated that intravenously administered ANP decreased the peak CK value by 20% compared with placebo,⁹ although this value did not reach significance because of the small number of patients and large standard deviation. The estimated percent reductions in Σ CK are 20% in the ANP treatment group and the standard deviation will be 5-fold larger than the mean value (>100%). There will be no changes in Σ CK in the placebo group. To detect statistically significant differences with 80% power and with $\alpha=0.05$, a total of 600 patients (300 patients per group) is required as $p=0.021$ with 10% dropout.

SNPs

It has been suggested that common genetic variants, such as SNPs, may influence the effectiveness of pharmacological therapy and patient susceptibility to disease.¹⁶ In the J-WIND-ANP, genotype distribution will be analyzed among the patients with ANP treatment and will be compared between normal subjects and AMI patients, using SNPs of genes that may modulate the functions of ANP and that may affect the metabolism of ANP in the patients. The association of SNPs of targeted genes with patient responsiveness to ANP treatment will be examined in patients by comparing them with normal subjects. Furthermore, the SNPs of genes that may influence the occurrence of AMI will be investigated in AMI patients by comparing them with normal subjects. The SNPs information of the control subjects comes from the data base of Japanese SNP (JSNP; <http://snp.ims.u-tokyo.ac.jp/index.html>) officially opened in Japan. Finally, we will also assess the association of clinical outcomes with therapeutic drug combination in regard to the drug-related SNPs, such as SNPs of calcium-channel-related genes for calcium channel blockers. We have a list of ANP-related, infarct-related, and drug-related genes, but because of the sensitive nature of the information, including patents for SNPs analysis, we are unable to disclose it.

Data Management

Data for CK and the LVG cinefilms are collected by Koteisyo-kyokai (Tokyo), the organization established by the Japanese government for promoting large-scale clinical trials of Medical Frontier Strategy Research using Health and Labor Sciences Research Grants. Koteisyo-kyokai helps to manage the randomization, registration, data collection, and data analysis of the patients in the J-WIND-ANP. We also established a system that completely protects the private information of patients who agreed to SNPs analysis. In brief, the blood sample is labeled with a temporal code provided from the J-WIND office, and then it is sent to SRL where the DNA is extracted from the sample. From SRL, the sample is sent to the Individual Data Manager in the National Cardiovascular Center. The manager replaces the temporal code with an anonymous one and the samples are then analyzed by the HuBIT company. The SNPs data from HuBIT for the samples labeled with an anonymous code are strictly managed by the Individual Data Manager; however, the Individual Data Manager can never link the patients and their SNPs information. We have restricted the use of SNPs information to those specific aims described in the informed consent. DNA from patients is discarded after completion of the analysis.

Statistical Analysis

Continuous variables are reported as means and standard deviations. Because the primary end-points are comparing (1) infarct size estimated by the AUC of CK (and CK-MB) and by troponin T, and (2) the improvement in the regional wall motion scores evaluated by LVG in the AMI patients with and without ANP treatments, a two-tailed Student's *t* test for unpaired data will be used. All significant tests will be 2-sided, with type I error rate $\alpha=0.05$. Survival rates and cardiac events will be analyzed by survival analysis. For each clinical event outcome, the variable for analysis will be the time period between the beginning of the treatment and the first occurrence of the event of interest. Event rates in the placebo and ANP-treated groups are compared by the log-rank test. These analyses will be done on an intention-to-treat basis. Worsening of anginal status is defined as a worsening of at least one class in the Canadian Cardiovascular Society Foundation classification of angina. Relative frequencies of reperfusion injury (malignant ventricular arrhythmia during reperfusion periods, re-elevation of ST-segment, worsening of chest pain) are compared by chi-square test.

For the analysis of SNPs, genotype distributions is analyzed among the patients in the ANP treatment group, and between normal subjects and AMI patients. Multiple logistic linear regression analysis is used to show the genotype distributions between the groups, and the adjusted odds ratios and their 95% confidence intervals will be calculated. Genotypes that may affect pharmacological dynamics will be also analyzed in patients enrolled in the J-WIND-ANP. The prevalence of genotypes will be expressed as percentage and will be analyzed by chi-square test.

Traditional statistical analysis cannot work with a database of observations consisting of clinical information and data mining is used in such cases.^{12,13} It is currently being used in a number of other industries, such as financial and chemical companies. Essentially, this method identifies the association rules and patterns that reveal the relationship

among different items. The patterns investigated can be patient characteristics, medication used, and patient outcomes. Once the patterns have been validated, the results can be used to develop decision trees for patient care. The data mining method is especially useful for finding trends in drug interactions. In the case of J-WIND-ANP, we will generate for each patient a set of all medications administered and the clinical outcome, and by applying data mining, we can assess the association rules indicating relationships between medication and clinical outcome.

Funding Source

J-WIND-ANP is supported by Grants for Comprehensive Research on Aging and Health (H13-21seiki (seikatsu)-23) in Health and Labour Sciences Research from the Ministry of Health, Labour and Welfare, Japan. The ANP used in J-WIND-ANP is provided from the J-WIND office to the participating hospitals. The patients registered in the study do not pay extra cost to participate. The study is designed, conducted, analyzed, and interpreted by the investigators entirely independent of all funding sources.

Conclusion

The results of J-WIND-ANP will provide important data on the effects of ANP as an adjunct to PCI for AMI patients. Furthermore, by analyzing the SNPs of genes associated with the responsiveness to ANP therapy, the occurrence of AMI, and pharmacological dynamics, tailor-made therapy for patients post-MI will be established. Finally, the first application of data mining to a cardiovascular trial will discover the optimal therapeutic combination for post-MI patients. The broad range of data obtained by J-WIND-ANP will allow comprehensive assessments of the potential benefits of ANP, tailor-made therapy and optimal therapeutic combinations for patients post-MI.

Acknowledgments

This study is supported by Grants on Comprehensive Research on Aging and Health (H13-21seiki (seikatsu)-23) in Health and Labour Sciences Research from Ministry of Health, Labour and Welfare, Japan.

We thank Ms Yukiko Hanemoto, Satomi Ihara, Etsuko Fukuda, Megumi Yokoi, Ayako Kameda, Hiroko Kawakita and Masami Yokoyama for their excellent assistance. We also thank Drs Hitonobu Tomoike, Soh-ichiro Kitamura and Kunio Miyatake at National Cardiovascular Center and Masatsugu Hori at Osaka University Graduate School for their encouragement and support.

References

1. Primary Angioplasty in Myocardial Infarction Study Group (Grines CL, Browne KF, Marco J, Rothbaum D, Stone GW, O'Keefe J, et al). A comparison of immediate angioplasty with thrombolytic therapy for myocardial infarction. *N Engl J Med* 1993; **328**: 673-679.
2. Sakurai K, Watanabe J, Iwabuchi K, Koseki Y, Kon-No Y, Fukuchi M, et al. Comparison of the efficacy of reperfusion therapies for early mortality from acute myocardial infarction in Japan. *Circ J* 2003; **67**: 209-214.
3. Lamas GA, Flaker GC, Mitchell G, Smith SC Jr, Gersh BJ, Wun CC, et al. Effect of infarct artery patency on prognosis after acute myocardial infarction. *Circulation* 1995; **92**: 1101-1109.
4. Verma S, Fedak PW, Weisel RD, Butany J, Rao V, Maitland A, et al. Fundamentals of reperfusion injury for the clinical cardiologist. *Circulation* 2002; **105**: 2332-2336.
5. Jonassen AK, Aasum E, Riemersma RA, Mjos OD, Larsen TS. Glucose-insulin-potassium reduces infarct size when administered during reperfusion. *Cardiovasc Drugs Ther* 2000; **14**: 615-623.
6. Marzilli M, Orsini E, Marraccini P, Testa R. Beneficial effects of intracoronary adenosine as an adjunct to primary angioplasty in acute myocardial infarction. *Circulation* 2000; **101**: 2154-2159.
7. Cody RJ, Atlas SA, Laragh JH, Kubo SH, Covit AB, Ryman KS, et al. Atrial natriuretic factor in normal subjects and heart failure patients. Plasma levels and renal, hormonal, and hemodynamic responses to peptide infusion. *J Clin Invest* 1986; **78**: 1362-1374.
8. Emori T, Hirata Y, Imai T, Eguchi S, Kanno K, Marumo F. Cellular mechanism of natriuretic peptides-induced inhibition of endothelin-1 biosynthesis in rat endothelial cells. *Endocrinology* 1993; **133**: 2474-2480.
9. Hayashi M, Tsutamoto T, Wada A, Maeda K, Mabuchi N, Tsutsui T, et al. Intravenous atrial natriuretic peptide prevents left ventricular remodeling in patients with first anterior acute myocardial infarction. *J Am Coll Cardiol* 2001; **37**: 1820-1826.
10. Kuga H, Ogawa K, Oida A, Taguchi I, Nakatsugawa M, Hoshi T, et al. Administration of atrial natriuretic peptide attenuates reperfusion phenomena and preserves left ventricular regional wall motion after direct coronary angioplasty for acute myocardial infarction. *Circ J* 2003; **67**: 443-448.
11. Kikuchi M, Nakamura M, Suzuki T, Sato M, Takino T, Hiramori K. Usefulness of carperitide for the treatment of refractory heart failure due to severe acute myocardial infarction. *Jpn Heart J* 2001; **42**: 271-280.
12. Fukuzawa S, Ozawa S, Inagaki M, Shimada K, Sugioka J, Tateno K, et al. Nicorandil affords cardioprotection in patients with acute myocardial infarction treated with primary percutaneous transluminal coronary angioplasty: Assessment with thallium-201/iodine-123 BMIPP dual SPECT. *J Nucl Cardiol* 2000; **7**: 447-453.
13. Kobayashi Y, Goto Y, Daikoku S, Itoh A, Miyazaki S, Ohshima S, et al. Cardioprotective effect of intravenous nicorandil in patients with successful reperfusion for acute myocardial infarction. *Jpn Circ J* 1998; **62**: 183-189.
14. Doddi S, Marathe A, Ravi SS, Torney DC. Discovery of association rules in medical data. *Med Inform Internet Med* 2001; **26**: 25-33.
15. Bate A, Lindquist M, Edwards IR, Orre R. A data mining approach for signal detection and analysis. *Drug Saf* 2002; **25**: 393-397.
16. Christenson RH, Vollmer RT, Ohman EM, Peck S, Thompson TD, Duh SH, et al. Relation of temporal creatine kinase-MB release and outcome after thrombolytic therapy for acute myocardial infarction: TAMI Study Group. *Am J Cardiol* 2000; **85**: 543-547.
17. Sheehan FH, Schofer J, Mathey DG, Kellett MA, Smith H, Bolson EL, et al. Measurement of regional wall motion from biplane contrast ventriculograms: A comparison of the 30 degree right anterior oblique and 60 degree left anterior oblique projections in patients with acute myocardial infarction. *Circulation* 1986; **74**: 796-804.
18. Deschepper CF, Boutin-Ganache I, Zahabi A, Jiang Z. In search of cardiovascular candidate genes: Interactions between phenotypes and genotypes. *Hypertension* 2002; **39**: 332-336.

Appendix 1

The following investigators and institutions are participating in the J-WIND-ANP study.

Principal Investigator

Masafumi Kitakaze, National Cardiovascular Center.

Steering Committee

Tetsuo Minamio, Research Resident of Japan Foundation for Aging and Health for Medical Frontier Strategy Research by Health and Labor Sciences Research Grants; Kim Jiyoung, National Cardiovascular Center; Masanori Asakura, Research Fellow of the Japan Society for the Promotion of Science for Young Scientists; Yasunori Shintani, Osaka University Graduate School of Medicine; Hiroshi Asanuma, Osaka University Graduate School of Medicine.

Safety and Data Monitoring Committee

Kazuhiro Sase, National Cardiovascular Center, Yukihiro Koretsune, Hideo Kusuoka, National Osaka Hospital, Takashi Washio, Osaka University Graduate School of Technology.

Individual Data Manager

Akiko Ogai, National Cardiovascular Center.

J-WIND Investigators

Principal investigators in the hospitals are indicated with asterisks.

Division of Cardiology, Tokuyama Central Hospital, Tokuyama, Yamaguchi: Takahiro Iwami, *Hiroshi Ogawa; Division of Cardiology, Department of Medicine, National Cardiovascular Center, Suita city, Osaka: Satoshi Yasuda, *Shunichi Miyazaki; Department of Cardiology, Hyogo Brain and Heart Center at Himeji, Himeji city, Hyogo: Junya Shite, *Teishi Kajiya; Division of Cardiology, Shinbeppu Hospital, Beppu city, Ohita: Hidenori Tanaka, *Natsuki Nakamura; Division of Cardiovascular Center, Kumamoto National Hospital, Kumamoto-city, Kumamoto: *Fujimoto Kazuteru; Division of Cardiology, Kawasaki Medical School, Kurashiki city, Okayama: Shuichiro Kaji, *Takashi Akasaka; The Depart-

ment of Internal Medicine, Cardiovascular Division, Hyogo College of Medicine, Nishinomiya city, Hyogo: Motomaru Masutani, *Tadaaki Iwasaki; Division of Cardiology, Osaka Prefectural Hospital, Osaka city, Osaka: Mitsutoshi Asai, *Moritake Hoki; Department of Cardiology, Uwajima City Hospital, Uwajima, Ehime: Jiroh Komatsu, *Kouki Watanabe; Division of Cardiology, Fukuyama Cardiovascular Hospital, Fukuyama, Hiroshima: Seiichi Haruta, *Hiroyuki Kohno; Intensive Care Unit, Chiba Hokusoh Hospital, Nippon Medical School, Inba-gun, Chiba: *Noritake Hata; Internal Medicine Second Division, Surugadai Nihon-University Hospital, Chiyoda-ku, Tokyo, Ken Nagao, *Katsuo Kanmatsuse; Department of Cardiology, Akane Foundation Tsuchiya General Hospital, Naka-Ku, Hiroshima: Hironori Ueda, *Yasuhiko Hayashi; The Division of Cardiology, Tohsei National Hospital,

*Hiroyuki Yokoyama; Department of Cardiovascular Medicine, Kumamoto University School of Medicine, Kumamoto-city, Kumamoto: Michihiro Yoshimura, *Hisao Ogawa; Cardiovascular Division, Osaka Police Hospital, Osaka city, Osaka: Atsushi Hirayama, *Kazuhiisa Kodama; Division of Cardiology, Yokohama City University Medical Center, Yokohama city, Kanagawa: Teruyasu Sugano, *Kazuo Kimura; Cardiovascular Division, Kansai Rosai Hospital, Amagasaki city, Hyogo: Ohnishi Toshinari, *Shinsuke Nanto; First Department of Internal Medicine, Nara Medical University, Kashihara city, Nara: Shiro Uemura, *Yoshihiko Saito; Second Department of Internal Medicine, University of Yamanashi, Nakakyoma county, Yamanashi: Ken Umetani, *Kiyotaka Kukiya

Rationale and Design of a Large-Scale Trial Using Nicorandil as an Adjunct to Percutaneous Coronary Intervention for ST-Segment Elevation Acute Myocardial Infarction

— Japan-Working Groups of Acute Myocardial Infarction for the Reduction of Necrotic Damage by a K-ATP Channel Opener (J-WIND-KATP) —

Tetsuo Minamino, MD; Kim Jiyoung, MD*; Masanori Asakura, MD**;
Yasunori Shintani, MD†; Hiroshi Asanuma, MD†; Masafumi Kitakaze, MD*;
the J-WIND Investigators

Background The benefits of percutaneous coronary intervention (PCI) in acute myocardial infarction (AMI) are limited by reperfusion injury. In animal models, nicorandil, a hybrid of an ATP-sensitive K⁺ (KATP) channel opener and nitrates, reduces infarct size, so the Japan-Working groups of acute myocardial infarction for the reduction of Necrotic Damage by a K-ATP channel opener (J-WIND-KATP) designed a prospective, randomized, multicenter study to evaluate whether nicorandil reduces myocardial infarct size and improves regional wall motion when used as an adjunctive therapy for AMI.

Methods and Results Twenty-six hospitals in Japan are participating in the J-WIND-KATP study. Patients with AMI who are candidates for PCI are randomly allocated to receive either intravenous nicorandil or placebo. The primary end-points are (1) estimated infarct size and (2) left ventricular function. Single nucleotide polymorphisms (SNPs) that may be associated with the function of KATP-channel and the susceptibility of AMI to the drug will be examined. Furthermore, a data mining method will be used to design the optimal combined therapy for post-myocardial infarction (MI) patients.

Conclusions It is intended that J-WIND-KATP will provide important data on the effects of nicorandil as an adjunct to PCI for AMI and that the SNPs information that will open the field of tailor-made therapy. The optimal therapeutic drug combination will also be determined for post-MI patients. (*Circ J* 2004; 68: 101–106)

Key Words: Acute myocardial infarction; Data mining; Nicorandil; Randomized clinical trial; SNPs

Reperfusion of the ischemic myocardium by percutaneous coronary intervention (PCI) reduces the size of the infarct and improves left ventricular function, both of which contribute to an improved clinical outcome for patients with acute myocardial infarction (AMI).^{1–3} However, in some patients who undergo reperfusion therapy, reperfusion per se adversely leads to tissue damage known as reperfusion injury.⁴ Several clinical trials targeting the prevention or reduction of reperfusion injury are now in progress^{5,6} and nicorandil, a hybrid of an adenosine triphosphate (ATP)-sensitive potassium (K⁺-ATP) channel opener and nitrates, is a promising candidate for

adjunctive therapy for AMI. In animal models, several studies, including ours, have demonstrated that nicorandil reduces the size of the myocardial infarct and improves post-ischemic left ventricular function.^{7,8} In the clinical setting, however, the beneficial effects of nicorandil have been tested in single center studies only and the number of patients has been relatively small.^{9,10} Thus, larger multicenter studies are needed to assess whether these experimental effects of nicorandil can translate into clinical benefits. Japan-Working groups of acute myocardial infarction for the reduction of Necrotic Damage by a K-ATP channel opener (J-WIND-KATP) is a prospective, randomized, multicenter study designed to evaluate the beneficial effects of nicorandil as an adjunctive therapy for AMI. In the J-WIND-KATP, in addition to examining the effects of nicorandil treatment on clinical outcomes, including infarct size and left ventricular regional function, the association between single nucleotide polymorphisms (SNPs) of genes that may potentially influence either KATP-channel function or metabolism of nicorandil and the responsiveness of nicorandil therapy will be analyzed. Further, by comparing the prevalence of SNPs of genes that may influence the occurrence of AMI between normal subjects and AMI patients enrolled in the J-WIND-KATP, we can genetically

(Received July 8, 2003; revised manuscript received October 21, 2003; accepted November 19, 2003)

Research Resident of Japan Foundation for Aging and Health for Medical Frontier Strategy Research by Health and Labor Sciences Research Grants; *Cardiovascular Division of Medicine, National Cardiovascular Center, Suita, **Research Fellow of the Japan Society for the Promotion of Science for Young Scientists and †Department of Internal Medicine and Therapeutics, Osaka University Graduate School of Medicine, Suita, Japan

Mailing address: Masafumi Kitakaze, MD, PhD, Cardiovascular Division of Medicine, National Cardiovascular Center, Suita 565-8565, Japan. E-mail: kitakaze@hsp.nccvc.go.jp

Table 1 Inclusion Criteria for J-WIND-KATP

1. Age 20–79 years
2. Chest pain of more than 30 min
3. 0.1 mV ST-segment elevation in 2 contiguous ECG leads
4. Admission to hospital within 12 h of symptom onset
5. First episode of AMI

Table 2 Exclusion Criteria for J-WIND-KATP

1. History of old myocardial infarction
2. Left main coronary artery stenosis
3. Severe liver and/or kidney dysfunction
4. Suspected aortic dissection
5. History of coronary artery bypass graft
6. History of allergic response to drugs

Table 3 Cessation Criteria for J-WIND-KATP

1. Patient's decision to cease attending the study
2. Prolonged hypotension
3. Difficulty in continuing in the study because of an adverse event
4. Patient who does not match the inclusion criteria after registration
5. Patient who meets exclusion criteria after registration

predict the patient population that has the highest risks of AMI.

In conjunction, we plan to use a data mining method to determine the best therapeutic combination for decreasing the risk for cardiac events in patients with post-myocardial infarction (MI) because this method is useful for discovering combinational information from a database that is too large for traditional statistical methods.^{12,13} In the most recent clinical studies, the effects of single medication on the end-points have been assessed with no consideration of the effects of the drug combination. In addition, by examining SNPs information of the genes that may affect pharmacodynamics and the association rules of therapeutic combination with clinical outcomes, we should be able to provide important information for 'tailor-made' therapy of post-MI patients.

Methods

Study Population

Patients are eligible when all the inclusion criteria are fulfilled (Table 1). The exclusion and cessation criteria are listed in Tables 2 and 3, respectively. All patients sign written informed consent twice: immediately after hospitalization and a few weeks later when patients could decide on study participation under less urgent conditions. The principle investigator of each participating hospital will be in charge of the written informed consent forms (Appendix 1). The patients registered in the J-WIND-KATP are not able to participate in other clinical studies. Patients enrollment started on 31 October 2001, and will continue until 30 September 2005. Enrolled patients will be followed until 30 September 2007.

Protocol (Fig 1)

Immediately after the diagnosis of AMI, patients are randomly assigned to either a nicorandil or saline group by means of sealed envelopes containing the randomization schedule that was generated by computer before the beginning of the study. Randomization blocks are prepared for each participating hospital. The physicians responsible for giving the treatment are unaware of the randomization schedule. We adopted the envelope method instead of central randomization for the following reasons.

(1) It is not unusual for AMI patients not to be registered on the Web if the hospital presentation is an emergency, especially around midnight.

(2) There are some hospitals where physicians can not easily access the Web in the emergency room.

In the nicorandil group, after a bolus injection of nicorandil (0.067 mg/kg), it is continuously infused intravenously at $1.67 \mu\text{g}\cdot\text{kg}^{-1}\cdot\text{min}^{-1}$ for 24 h. In the control group, saline is continuously infused at the corresponding dose in the same manner. Accordingly, most patients enrolled in J-WIND-KATP start to receive nicorandil before recanalization. The study protocol does not restrict or specify any other diagnostic or therapeutic strategies, including the recanalization method such as percutaneous transluminal coronary angiography or thrombolytic therapy. Blood samples for creatine kinase (CK) and CK-MB measurements are drawn before the procedure and at 1, 2, 6, 9, 12, 18, 24, 36, 48 and 72 h after reperfusion.¹⁴ Troponin T is measured 15 and 96 h after symptom onset. The right anterior oblique

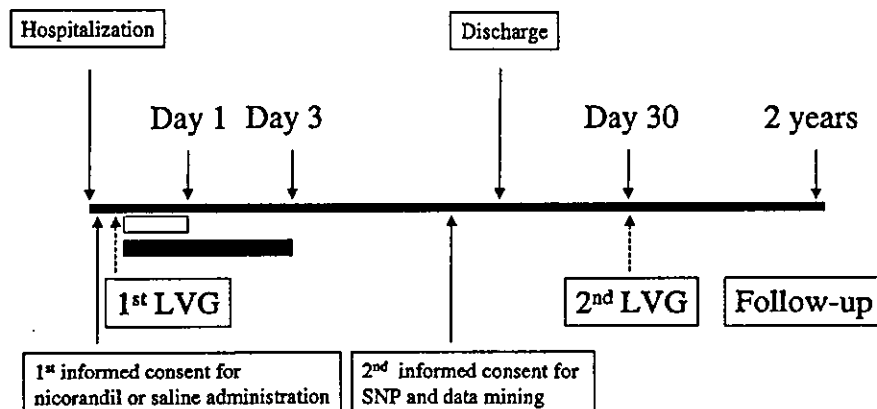


Fig 1. Overview of the J-WIND-KATP protocol. (White box) Nicorandil administration; (Black box) CK measurement.

Table 4 Drug List for Data Mining

Angiotensin converting enzyme inhibitors:
 Cilazapril Temocapril hydrochloride Perindopril erbumi
 Imidapril hydrochloride Enalapril maleate
 Others: _____ dose ____ mg

Angiotensin II type I receptor antagonists:
 Valsartan Candesartan cilexetil Losartan potassium
 Others: medication _____ dose ____ mg

Statins:
 Pravastatin sodium Atorvastatin calcium Simvastatin
 Fluvastatin sodium
 Others: _____ dose ____ mg

Ca channel blockers:
 Nifedipine Benidipine hydrochloride Amlodipine besilate
 Others: _____ dose ____ mg

β -blockers:
 Carvedilol Celiprolol hydrochloride Metoprolol tartrate Bisoprolol fumarate
 Others: medication _____ dose ____ mg

Anti-platelet drugs:
 Aspirin Ticlopidine hydrochloride Cilostazol
 Others: _____ dose ____ mg

Diuretics:
 Spironolactone Azosemide Furosemide
 Others: _____ dose ____ mg

Nitrates:
 Isosorbide mononitrate Nitrol-R Frandol Nitroglycerin
 Others: _____ dose ____ mg

Inotropic agents:
 Pimobendan Digitalis Docarpamine
 Others: _____ dose ____ mg

Adenosine re-uptake inhibitors: KATP channel opener
 Dipyridamole mg Nicorandil ____ mg

Anti-arrhythmic agents:
 Amiodarone Pilsicainide Propafenone Mexiletine
 Disopyramide
 Others: _____ dose ____ mg

Anti-diabetic agents:
 Glimicron Euglucon Voglibose Acarbose
 Pioglitazone
 Others: _____ dose ____ mg

Other medication:

views of left ventriculogram (LVG) are analyzed in the acute phase and approximately 1 month later (2–6 weeks). End-diastolic volume and ejection fraction are measured by the area–length method. The regional wall motion (standard deviation per chord) of the area of the targeted artery is analyzed with the centerline method.⁵ Two angiographers who are unaware of the patients' allocation independently analyze the cinefilms.

After the completion of intensive care for AMI, patients are treated with cardiovascular drugs. We ask the participating physicians to select from the drugs listed in Table 4 in order to limit the number of drugs to be included in the data mining. Furthermore, once the drugs for each patient are decided, we ask the physicians not to change them for 2 years unless the patient's condition dictates a revision of therapy. By finding the association rules between the effectiveness of a set of treatments and clinical outcomes in patients with post-MI, we can identify the optimal therapeutic combination for these patients.

A blood sample for SNPs is drawn before discharge from patients with signed written informed consent. After extraction of the DNA of the sample, SNPs will be exam-

ined for the targeted genes that (1) influence the occurrence of AMI, (2) modulate the function and/or metabolism of nicorandil, and (3) affect the pharmacological dynamics of the drugs listed in Table 4. The protocol of the J-WIND-KATP, including SNPs analysis, has been approved by the institutional review board and ethical committees of all hospitals involved. A counseling system to respond to the questions and requirements of the registered patients about the gene analysis has been established in the National Cardiovascular Center.

End-Points

The primary end-points are (1) estimated infarct size and (2) left ventricular function (left ventricular ejection fraction and end-diastolic volume) and regional wall motion. The infarct size is estimated by 2 methods: the area under the curve (AUC) of CK (and CK-MB) and a single measurement of troponin T.⁴ Left ventricular function and regional wall motion are evaluated by LVG that is performed at the time of hospital admission and 2–6 weeks later.⁵ The secondary end-points are (1) survival rate, (2) cardiovascular events (ie, cardiac death, nonfatal re-infarct-

tion, re-hospitalization because of cardiac disease, revascularization), (3) reperfusion injury (ie, malignant ventricular arrhythmia during reperfusion periods, re-elevation of ST-segment, worsening of chest pain), and (4) an association of SNPs of KATP-channel related genes with responsiveness to nicorandil treatment. SNPs of genes that may influence the occurrence of AMI are compared between patients enrolled in the J-WIND-KATP and normal subjects. In addition, the optimal combination of therapeutic drugs to treat patients post-MI will be retrospectively surveyed by data mining. Clinical characteristics and medication during the follow-up period must be reported to the J-WIND-KATP Data and Safety Committee at 3, 6, 12 and 24 months after registration.

Safety

The Safety and Data Monitoring Committee, comprising 3 physicians and a statistician not involved in the conduct of the trial, monitors all adverse events. Furthermore, research nurses visit the participating hospitals to check that the registration, administration of drugs and data collection are correctly performed according to the protocol. Interim analyses of study data will be performed when approximately 20%, 40%, and 60% of the expected number of patients have been enrolled. The committee members do not communicate any results to the Steering Committee, unless discontinuation of the study is recommended.

Sample Size

A previous single center study demonstrated that intravenously administered nicorandil decreased the peak CK value by 20% compared with placebo,⁹ although this value did not reach significance because of the small number of patients and large standard deviation. The estimated percent reductions in Σ CK are 20% in the nicorandil treatment group and the standard deviation will be 5-fold larger than the mean value (>100%). There will be no changes in Σ CK in the placebo group. To detect statistically significant differences with 80% power and with $\alpha=0.05$, a total of 600 patients (300 patients per group) is required as $p=0.021$ with 10% dropout.

SNPs

It has been suggested that common genetic variants, such as SNPs, may influence the effectiveness of pharmacological therapy and patient susceptibility to disease.¹⁶ In the J-WIND-KATP, genotype distribution will be analyzed among the patients in the nicorandil treatment group and will be compared between normal subjects and AMI patients, using SNPs of genes that may modulate the functions of the KATP-channel and may affect the metabolism of nicorandil in patients. The association of SNPs of targeted genes with patient responsiveness to nicorandil treatment will be examined in patients by comparing them with normal subjects. Furthermore, the SNPs of genes that may influence the occurrence of AMI will be investigated in AMI patients by comparing them with normal subjects. The SNPs information of the control subjects comes from the data base of Japanese SNP (JSNP: <http://snp.ims.u-tokyo.ac.jp/index.html>) officially opened in Japan. Finally, we will also assess the association of clinical outcomes with therapeutic drug combination in regard to the drug-related SNPs, such as SNPs of calcium-channel-related genes for calcium channel blockers. We have a list of K-ATP channels-related, infarct-related, and drug-related genes, but

because of the sensitive nature of the information, including patents for SNPs analysis, we are unable to disclose it.

Data Management

Data for CK and the LVG cinefilms are collected by Koteisyo-kyokai (Tokyo), the organization established by the Japanese government for promoting large-scale clinical trials of Medical Frontier Strategy Research using Health and Labor Sciences Research Grants. Koteisyo-kyokai helps to manage the randomization, registration, data collection, and data analysis of the patients in the J-WIND-KATP. We also established a system that completely protects the private information of patients who agreed to SNPs analysis. In brief, the blood sample is labeled with a temporal code provided from the J-WIND office, and then it is sent to SRL where the DNA is extracted from the sample. From SRL, the sample is sent to the Individual Data Manager in the National Cardiovascular Center. The manager replaces the temporal code with an anonymous one and the samples are then analyzed by the HuBIT company. The SNPs data from HuBIT for the samples labeled with an anonymous code are strictly managed by the Individual Data Manager; however, the Individual Data Manager can never link the patients and their SNPs information. We have restricted the use of SNPs information to those specific aims described in the informed consent. DNA from patients is discarded after completion of the analysis.

Statistical Analysis

Continuous variables are reported as means and standard deviations. Because the primary end-points are comparing (1) infarct size estimated by the AUC of CK (and CK-MB) and by troponin T, and (2) the improvement in the regional wall motion scores evaluated by LVG in the AMI patients with and without nicorandil treatments, a two-tailed Student's *t* test for unpaired data will be used. All significance tests will be 2-sided, with type I error rate $\alpha=0.05$. Survival rates and cardiac events will be analyzed by survival analysis. For each clinical event outcome, the variable for analysis will be the time period between the beginning of the treatment and the first occurrence of the event of interest. Event rates in the placebo and nicorandil-treated groups are compared by the log-rank test. These analyses will be done on an intention-to-treat basis. Worsening of anginal status is defined as a worsening of at least one class in the Canadian Cardiovascular Society Foundation classification of angina. Relative frequencies of reperfusion injury (malignant ventricular arrhythmia during reperfusion periods, re-elevation of ST-segment, worsening of chest pain) are compared by chi-squared test.

For the analysis of SNPs, genotype distributions is analyzed among the patients in the nicorandil treatment group, and between normal subjects and AMI patients. Multiple logistic linear regression analysis is used to show the genotype distributions between the groups, and the adjusted odds ratios and their 95% confidence intervals will be calculated. Genotypes that may affect pharmacological dynamics will be also analyzed in patients enrolled in the J-WIND-KATP. The prevalence of genotypes will be expressed as percentage and will be analyzed by chi-square test.

Traditional statistical analysis cannot work with a database of observations consisting of clinical information and data mining is used in such cases.^{12,13} It is currently being

used in a number of other industries, such as financial and chemical companies. Essentially, this method identifies the association rules and patterns that reveal the relationship among different items. The patterns investigated can be patient characteristics, medication used, and patient outcomes. Once the patterns have been validated, the results can be used to develop decision trees for patient care. The data mining method is especially useful for finding trends in drug interactions. In the case of J-WIND-KATP, we will generate for each patient a set of all medications administered and the clinical outcome, and by applying data mining, we can assess the association rules indicating relationships between medication and clinical outcome.

Funding Source

J-WIND-KATP is supported by Grants for Comprehensive Research on Aging and Health (H13-21seiki (seikatsu)-23) in Health and Labour Sciences Research from the Ministry of Health, Labour and Welfare, Japan. The nicorandil used in the J-WIND-KATP is provided from the J-WIND office to the participating hospitals. The patients registered in the study do not pay extra cost to participate. The study is designed, conducted, analyzed, and interpreted by the investigators entirely independent of all funding sources.

Conclusion

The results of J-WIND-KATP will provide important data on the effects of nicorandil as an adjunct to PCI for AMI patients. Furthermore, by analyzing the SNPs of genes associated with the responsiveness to nicorandil therapy, the occurrence of AMI, and pharmacological dynamics, tailor-made therapy for patients post-MI will be established. Finally, the first application of data mining to a cardiovascular trial will discover the optimal therapeutic combination for post-MI patients. The broad range of data obtained by J-WIND-KATP will allow comprehensive assessments of the potential benefits of nicorandil, tailor-made therapy and optimal therapeutic combinations for patients post-MI.

Acknowledgments

This study is supported by Grants on Comprehensive Research on Aging and Health (H13-21seiki(seikatsu)-23), in Health and Labour Sciences Research from Ministry of Health, Labour and Welfare, Japan.

We thank Ms Yukiko Hanemoto, Satomi Ihara, Eisuko Fukuda, Megumi Yokoi, Ayako Kameda, Hiroko Kawakita and Masami Yokoyama for their excellent assistance. We also thank Drs Hitonobu Tomoike, Soh-ichiro Kitamura and Kunio Miyatake at the National Cardiovascular Center and Masatsugu Hori at Osaka University Graduate School for their encouragement and support.

References

1. Primary Angioplasty in Myocardial Infarction Study Group (Grines CL, Browne KF, Marco J, Rothbaum D, Stone GW, O'Keefe J, et al). A comparison of immediate angioplasty with thrombolytic therapy for myocardial infarction. *N Engl J Med* 1993; **328**: 673-679.
2. Sakurai K, Watanabe J, Iwabuchi K, Koseki Y, Kon-No Y, Fukuchi M, et al. Comparison of the efficacy of reperfusion therapies for early mortality from acute myocardial infarction in Japan. *Circ J* 2003; **67**: 209-214.
3. Lamas GA, Flaker GC, Mitchell G, Smith SC Jr, Gersh BJ, Wun CC, et al. Effect of infarct artery patency on prognosis after acute myocardial infarction. *Circulation* 1995; **92**: 1101-1109.
4. Verma S, Fedak PW, Weisel RD, Butany J, Rao V, Maitland A, et al. Fundamentals of reperfusion injury for the clinical cardiologist. *Circulation* 2002; **105**: 2332-2336.
5. Jonassen AK, Aasum E, Riemersma RA, Mjos OD, Larsen TS. Glucose-insulin-potassium reduces infarct size when administered during reperfusion. *Cardiovasc Drugs Ther* 2000; **14**: 615-623.
6. Marzilli M, Orsini E, Marraccini P, Testa R. Beneficial effects of intracoronary adenosine as an adjunct to primary angioplasty in acute myocardial infarction. *Circulation* 2000; **101**: 2154-2159.
7. Kitakaze M, Minamino T, Node K, Komamura K, Shinozaki Y, Chujo M, et al. Role of activation of ectosolic 5'-nucleotidase in the cardioprotection mediated by opening of K⁺ channels. *Am J Physiol* 1996; **270**: H1744-H1756.
8. Mizumura T, Nithipatikom K, Gross GJ. Infarct size-reducing effect of nicorandil is mediated by the KATP channel but not by its nitrate-like properties in dogs. *Cardiovasc Res* 1996; **32**: 274-285.
9. Sugimoto K, Ito H, Iwakura K, Ikushima M, Kato A, Kimura R, et al. Intravenous nicorandil in conjunction with coronary reperfusion therapy is associated with better clinical and functional outcomes in patients with acute myocardial infarction. *Circ J* 2003; **67**: 295-300.
10. Fukuzawa S, Ozawa S, Inagaki M, Shimada K, Sugioka J, Tateno K, et al. Nicorandil affords cardioprotection in patients with acute myocardial infarction treated with primary percutaneous transluminal coronary angioplasty: Assessment with thallium-201/iodine-123 BMIPP dual SPECT. *J Nucl Cardiol* 2000; **7**: 447-453.
11. Kobayashi Y, Goto Y, Daikoku S, Itoh A, Miyazaki S, Ohshima S, et al. Cardioprotective effect of intravenous nicorandil in patients with successful reperfusion for acute myocardial infarction. *Jpn Circ J* 1998; **62**: 183-189.
12. Doddi S, Marathe A, Ravi SS, Torney DC. Discovery of association rules in medical data. *Med Inform Internet Med* 2001; **26**: 25-33.
13. Bate A, Lindquist M, Edwards IR, Orre R. A data mining approach for signal detection and analysis. *Drug Saf* 2002; **25**: 393-397.
14. Christenson RH, Vollmer RT, Ohman EM, Peck S, Thompson TD, Duh SH, et al. Relation of temporal creatine kinase-MB release and outcome after thrombolytic therapy for acute myocardial infarction: TAMI Study Group. *Am J Cardiol* 2000; **85**: 543-547.
15. Sheehan FH, Schofer J, Mathey DG, Kellett MA, Smith H, Bolson EL, et al. Measurement of regional wall motion from biplane contrast ventriculograms: A comparison of the 30 degree right anterior oblique and 60 degree left anterior oblique projections in patients with acute myocardial infarction. *Circulation* 1986; **74**: 796-804.
16. Deschepper CF, Boutin-Ganache I, Zahabi A, Jiang Z. In search of cardiovascular candidate genes: Interactions between phenotypes and genotypes. *Hypertension* 2002; **39**: 332-336.

Appendix 1

The following investigators and institutions are participating in the J-WIND-KATP study.

Principle Investigator

Masafumi Kitakaze, National Cardiovascular Center.

Steering Committee

Tetsuo Minamio, Research Resident of Japan Foundation for Aging and Health for Medical Frontier Strategy Research by Health and Labor Sciences Research Grants; Kim Jiyoung, National Cardiovascular Center; Masanori Asakura, Research Fellow of the Japan Society for the Promotion of Science for Young Scientists; Yasunori Shintani, Osaka University Graduate School of Medicine; Hiroshi Asanuma, Osaka University Graduate School of Medicine.

Safety and Data Monitoring Committee

Kazuhiro Sase, National Cardiovascular Center; Yukihiko Koretsune, Hideo Kusuoka, National Osaka Hospital, Takashi Washio, Osaka University Graduate School of Technology.

Individual Data Manager

Akiko Ogai, National Cardiovascular Center.

J-WIND Investigators

Principal investigators in the hospitals are indicated with asterisks. Department of Cardiology, Ehime National Hospital, Osen-gun, Ehime: Takashi Otani, *Michihito Sekiya; Division of Cardiology, Funabashi, Municipal Medical Center, Funabashi, Chiba: Kazuhiro Shimada, *Shigeru Fukuzawa; Department of Cardiology, Rinku General Medical Center, Izumisano, Osaka: Yuji Yasuga, *Yoshiyuki Nagai; Division of Cardiology, Saiseikai Fukuoka General Hospital, Fukuoka city, Fukuoka: Yutaka Akatuka, *Yusuke Yamamoto; Division of Cardiology, Tokushima Red Cross Hospital, Komatsushima, Tokushima: Takefumi Takahashi, *Yoshikazu Hiasa; Department of Cardiology, Hiroshima City Hospital, Naka-Ku, Hiroshima: Ichiro Inoue, *Masaharu Ishihara; Department of Cardiology, Kyushu Kosei Nenkin Hospital, Kitakyushu city, Fukuoka: Masao Takemoto, *Hideo Yamamoto; Division of Cardiology, Miki City Hospital, Miki, Hyogo: *Kojiro Awano; Department of Cardiology, Kameda Medical Center, Kamogawa city, Chiba: Akihiko Matsumura, *Yuji Hashimoto; Division of Cardiology, St Mary's Hospital, Kurume

city, Fukuoka: Seiki Harada, *Kunihiko Yamamoto; Department of Cardiology, Chiba Emergency Medical Center, Chiba city, Chiba: *Iwao Ishibashi; Department of Cardiology, Musashino Red Cross Hospital, Musashino city, Tokyo: Tohru Obayashi, *Akihiro Niwa; Department of Cardiology, Ogaki Municipal Hospital, Ogaki city, Gifu: Tomohiro Kono, *Takahito Sone; Shizuoka Prefectural General Hospital, Shizuoka city, Shizuoka: Kazuhiko Ohbayashi, *Osamu Doi; Division of Cardiology, Department of Internal Medicine, Kobe City General Hospital, Kobe city, Hyogo: Atsushi Yamamuro, *Kenichi Shiratori; Division of Cardiology, Sakurabashi Watanabe Hospital, Osaka, Osaka: Hiroshi Ito, *Kenshi Fujii; Department of Cardiovascular Medicine, Kyushu University Faculty of Medicine, Higashi-ku, Fukuoka: Yoji Hirakawa, *Kensuke Egashira; Department of Cardiology, Kanazawa Medical University Hospital, Kahoku County, Ishikawa: Shinji Okubo, *Noboru Takekoshi; Department of Cardiology, Kawachi General Hospital, Higashiosaka-city,

Osaka: Sadao Yoshida, *Masayoshi Mishima; Department of Cardiology, Cardiovascular Center, Omura Municipal Hospital, Omura city, Nagasaki: *Yoshito Tanioka; Department of Cardiovascular Medicine, Matsuyama Shimin Hospital, Matsuyama city, Ehime: Hiroyuki Fujieda, *Mitsunori Abe; Department of Cardiology, Sasebo Municipal General Hospital, Sasebo city, Nagasaki: Kohsuke Shioguchi, *Toshihiko Yamasa; Center for Cardiovascular Interventions, Chiba University Hospital, Chuo-ku, Chiba: Nobuyuki Komiyama, *Issei Komuro; Cardiovascular Division of Medicine, Nagasaki Municipal Hospital, Nagasaki-city, Nagasaki: Hiroshi Nakashima, *Shin Suzuki; Second Department of Internal Medicine, Tokyo Medical University Hospital, Shinjuku-ku, Tokyo: Nobuhiro Tanaka, *Akira Yamashina; Department of Cardiology, Tokyo Metropolitan Bokuto General Hospital, Sumida-Ku, Tokyo: Toru Iwama, *Ichiro Kubo; Department of Cardiovascular medicine, Hokkaido Cardiovascular Hospital, Sapporo city, Hokkaido; Masaru Yamaki, *Naoki Funayama.

Ablation of MEK Kinase 1 Suppresses Intimal Hyperplasia by Impairing Smooth Muscle Cell Migration and Urokinase Plasminogen Activator Expression in a Mouse Blood-Flow Cessation Model

Yan Li, MD, PhD*; Tetsuo Minamino, MD, PhD*; Osamu Tsukamoto, MD*; Toshiaki Yujiri, MD, PhD; Yasunori Shintani, MD; Ken-ichiro Okada, MD; Yoko Nagamachi, BS; Masashi Fujita, MD; Akio Hirata, MD; Shoji Sanada, MD, PhD; Hiroshi Asanuma, MD, PhD; Seiji Takashima, MD, PhD; Masatsugu Hori, MD, PhD; Gary L. Johnson, PhD; Masafumi Kitakaze, MD, PhD

Background—Migration, proliferation, and matrix-degrading protease expression of smooth muscle cells (SMCs) are major features of intimal hyperplasia after vascular injury. Although MEK kinase 1 (MEKK1) has been shown to regulate cell migration and urokinase plasminogen activator (uPA) expression, the precise role of MEKK1 in this process remains unknown.

Methods and Results—We triggered a vascular remodeling model by complete ligation of the right common carotid artery in wild-type (WT) and MEKK1-null (MEKK1^{-/-}) mice. The intimal areas 28 days after ligation were significantly decreased in the ligated MEKK1^{-/-} arteries compared with WT arteries (28±8 versus 65±17 μm², *P*<0.05). There were no differences in the ratios of proliferating cell nuclear antigen (PCNA)-positive cells to total cells within the arterial wall between WT and MEKK1^{-/-} arteries. Proliferation capacity also did not differ between WT and MEKK1^{-/-} cultured aortic smooth muscle cells (AoSMCs). In contrast, the number of intimal PCNA-positive cells 7 days after ligation was significantly smaller in MEKK1^{-/-} arteries. Three different migration assays revealed that migration and invasion of MEKK1^{-/-} AoSMCs were markedly impaired. Addition of full-length MEKK1 restored the migration capacity of MEKK1^{-/-} AoSMCs. The number of MEKK1^{-/-} AoSMCs showing lamellipodia formation by epithelial growth factor was significantly smaller compared with those of WT SMCs. Furthermore, uPA expression after ligation was markedly decreased in MEKK1^{-/-} arteries.

Conclusions—MEKK1 is implicated in vascular remodeling after blood-flow cessation by regulating the migration and uPA expression of SMCs. MEKK1 is a potential target for drug development to prevent vascular remodeling. (*Circulation*. 2005;111:1672-1678.)

Key Words: remodeling ■ muscle, smooth ■ vasculature ■ restenosis

Blood vessels respond to damaging stimuli by activating a remodeling mechanism that leads to intimal hyperplasia.^{1,2} Accumulating evidence has shown that the underlying causes of intimal hyperplasia are the invasion and proliferation of vascular smooth muscle cells (SMCs), both of which processes are triggered and controlled by numerous growth factors and mitogens.² Cell invasion involves migration by cytoskeletal reorganization³ and activation of a cascade of proteases that degrade various extracellular matrix (ECM) components.² Urokinase-type plasminogen activator (uPA) is

responsible for degradation of the ECM.⁴ Recent studies in uPA-deficient mice have demonstrated that the number of neointimal SMCs after injury is markedly reduced compared with those in wild-type (WT) mice, suggesting that uPA plays a critical role in cell invasion during vascular remodeling.⁵

MEK kinase 1 (MEKK1) is a 196-kDa, mitogen-activated protein kinase kinase kinase (MAP3K) that acts as an upstream regulator of several MAPK pathways.⁶⁻⁸ MEKK1 has been implicated in diverse and cell type-specific biological responses, including cardiac hypertrophy,⁶ cell survival,⁷

Received August 26, 2004; revision received November 16, 2004; accepted November 18, 2004.

From the Department of Internal Medicine and Therapeutics (Y.L., T.M., O.T., Y.S., K.-i.O., Y.N., M.F., A.H., S.S., H.A., S.T., M.H.), Osaka University Graduate School of Medicine, Suita, Osaka, Japan; the Department of Cardiovascular Medicine (M.K.), National Cardiovascular Center, Suita, Osaka, Japan; the Department of Cardiology (Y.L.), Xijing Hospital, Forth Military Medical University, Xi'an, People's Republic of China; the Department of Bio-Signal Analysis (T.Y.), Yamaguchi University Graduate School of Medicine, Ube, Yamaguchi, Japan; and the Department of Pharmacology (G.L.J.), University of North Carolina School of Medicine, Chapel Hill, NC.

*Drs Li, Minamino, and Tsukamoto contributed equally to this work.

Correspondence to Tetsuo Minamino, MD, PhD, Division of Cardiology, Department of Internal Medicine and Therapeutics, Osaka University Graduate School of Medicine, 2-2 Yamadaoka, Suita, Osaka 565-0871, Japan. E-mail minamino@medone.med.osaka-u.ac.jp

© 2005 American Heart Association, Inc.

Circulation is available at <http://www.circulationaha.org>

DOI: 10.1161/01.CIR.0000160350.20810.0F

and apoptosis.⁸ Recent studies on MEKK1-null (MEKK1^{-/-}) mice have uncovered a unique function for this protein kinase in cell migration.^{9,10} MEKK1^{-/-} mice were found to exhibit impairment of embryonic eyelid closure, a process involving epithelial cell migration.⁹ MEKK1 is also involved in growth factor-induced embryonic stem cell migration and contributes to fibroblast and epithelial cell migration *in vitro*.¹⁰ Furthermore, endogenous and overexpressed MEKK1 was reported to colocalize with the α -actinin cytoskeleton along actin stress fibers in focal adhesions.¹¹ Conversely, cytoskeletal reorganization can also lead to MEKK1 activation.¹² This close relationship between MEKK1 and the cytoskeleton implies that MEKK1 may be essential for regulating morphological changes such as the formation of lamellipodia, which proceeds to cell migration.^{3,13,14} Furthermore, MEKK1 is necessary for uPA upregulation in response to fibroblast growth factor-2 (FGF-2).¹⁵ These findings indicate that MEKK1 might play an important role in SMC migration and uPA production, both of which will affect SMC invasion during vascular remodeling. Herein, using a blood-flow cessation model in mice with targeted ablation of the *MEKK1* gene, we tested our hypothesis that MEKK1 plays a pivotal pathophysiological role in arterial remodeling by regulating SMC migration and uPA expression.

Methods

Animals and Blood-Flow Cessation Model

All animal studies were conducted in accordance with guidelines of the National Institutes of Health (Bethesda, Md) and institutional Animal Care and Use Committees. MEKK1^{-/-} mice were generated as described previously.⁹ The blood-flow cessation model was performed as reported previously.¹⁶ Carotid arteries were harvested immediately for biochemical analysis or after fixation for morphological and immunohistological analysis 1, 3, 7, and 28 days after surgery.

Morphometric and Histological Examinations

Standard hematoxylin-eosin staining, elastica van Gieson's staining, immunostaining for uPA (1:100, American Diagnostica), and proliferating cell nuclear antigen (PCNA) staining (1:50, Santa Cruz) were performed on serial sections (5 μ m) within 0.5 mm proximal to the site of ligation of right common carotid arteries, as reported previously.^{17,18} The luminal, internal elastic lamina (IEL), and external elastic lamina areas were measured with Scion Image software (Scion Corp). Morphological parameters were calculated as described previously.¹⁹ In brief, the intimal area was calculated as the IEL area minus luminal area, and the medial area was the external elastic lamina area minus IEL area. The ratio of intima to media area (I/M) was calculated as intimal area/medial area, and the stenotic ratio was calculated as the intimal area/IEL area \times 100.

Primary Culture of AoSMCs and Transfection

Primary culture of aortic SMCs (AoSMCs) was performed and characterized as described previously.²⁰ Cells were identified by positive immunostaining for α -smooth muscle actin (American Research Products). AoSMCs were transiently transfected with lipofectamine and either a full-length form of MEKK1 vector (MEKK1FL) or an empty vector (pcDNA3.1).²¹ After 48 hours, SMCs were studied in migration assays or for uPA expression.

AoSMC Proliferation Assay

AoSMCs (5×10^3) were cultured for 24 hours in 96-well plates with or without epithelial growth factor (EGF, 20 ng/mL), FGF-2 (20 ng/mL, R&D Systems, Inc), or platelet-derived growth factor-BB

(PDGF-BB, 25 ng/mL, Sigma). Then, [³H]thymidine incorporation and cell number were measured, as previously reported.²²

Quantification of Scrape Wound-Induced Migration Assay

Dense monolayers of overconfluent AoSMCs grown on Laboratory-Tek chamber slides were scraped with a sterile scraper as described previously.²³ After the wound was created, cells were incubated for 24 hours with or without FGF-2 (20 ng/mL) and visualized with rhodamine-phalloidin (R-451, Molecular Probes). The number of and distance that AoSMCs migrated from the wound line were calculated as the mean of 6 different fields.

Aortic Explant Migration Assay

Preparation of aortic explants was performed as described previously.²⁴ Explants were counted as positive when >1 cell was observed and identified by positive staining for α -smooth muscle actin.

Transwell Matrigel-Coated Chamber Invasion Assay

Cell invasion was analyzed with a BioCoat Matrigel invasion chamber (BD Biosciences Corp), as described previously.²⁵ Inserts without a Matrigel coating were used as controls. FGF-2 (20 ng/mL) was added to the lower chambers as a chemoattractant. The number of invading cells was manually counted per high-power field for each condition (10 fields for each filter). The percentage of invasion was calculated as (invading cells in Matrigel inserts/migrated cells of control inserts) \times 100.

Immunofluorescence Confocal Microscopy

Immunofluorescence staining with rhodamine-phalloidin and a monoclonal antibody for uPA (1:50) was performed as described previously.²⁶ Staining was examined with a Nikon Eclipse TE2000-U confocal scanning electron microscope.

Protein Extraction and Western Blotting Analysis

Protein extraction and immunoblotting were performed as described previously.^{15,21,22} Protein phosphorylation levels were normalized to the matching densitometric values of nonphosphorylated proteins.

Statistical Analysis

All data were expressed as mean \pm SEM. Significant differences were analyzed by an unpaired Student *t* test, Fisher exact test, or ANOVA followed by the Bonferroni post hoc test. A value of $P < 0.05$ was considered statistically significant.

Results

MEKK1 Ablation Inhibits Intimal Hyperplasia

There was no intimal thickening in unligated arteries of either WT or MEKK1^{-/-} mice. Significant neointimal growth was observed 28 days after ligation in WT mice, whereas it was much less in MEKK1^{-/-} mice (Figure 1A). Morphometric analysis of ligated arteries on day 28 revealed that the average intimal area was significantly smaller in MEKK1^{-/-} mice than in WT mice, whereas no difference in medial area was observed between WT and MEKK1^{-/-} mice (Figure 1B). Consequently, I-M ratios and stenotic ratios were significantly decreased in MEKK1^{-/-} mice compared with those in WT mice (Figure 1B).

MEKK1 Ablation Prevented Increases in the Numbers of Intimal PCNA-Positive Cells

In both WT and MEKK1^{-/-} mice, the ratios of PCNA-positive cells to total cells within the arterial wall, intima, and media were significantly increased 3 days after ligation

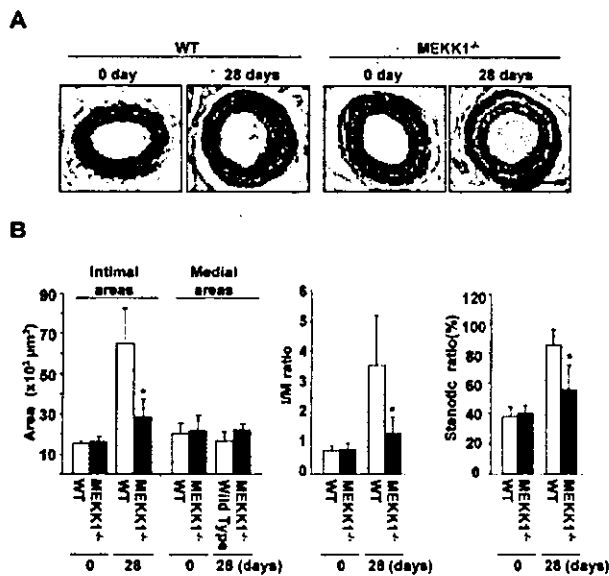


Figure 1. Photomicrographs and morphometry of intimal formation after ligation of carotid arteries. **A**, Representative cross sections of unligated and ligated carotid arteries on day 28 (elastica van Gieson's stain). Bar indicates 100 μm . **B**, Quantitative analysis of intimal and medial areas, I-M ratio, and stenotic ratio of ligated arteries. * $P < 0.05$ vs WT mice.

compared with those 1 day after ligation, but there were no significant differences between WT and MEKK1^{-/-} mice. It is noteworthy that 7 days after ligation, the number of PCNA-positive cells in the intima was significantly less in MEKK1^{-/-} arteries than in WT arteries, although there was no difference within other areas (Figure 2A and 2B). These findings suggest that migration of PCNA-positive cells from the media to the intima was impaired, whereas proliferation was not impaired in MEKK1^{-/-} mice. Consistent with *in vivo* data, no difference was observed in [³H]thymidine incorporation and cell number between WT and MEKK1^{-/-} AoSMCs after stimulation with PDGF-BB *in vitro* (Figure 2C). Treatment with EGF or FGF-2 instead of PDGF-BB yielded identical results (data not shown).

Effects of Ablation of MEKK1 on MAPK Activities of AoSMCs

Ablation of MEKK1 does not affect the total protein expression of extracellular signal-regulated kinase (ERK), c-Jun NH₂-terminal kinase (JNK), or p38. We examined the effects of ablation of MEKK1 on MAPK activities of AoSMCs. FGF-2-induced JNK and ERK but not p38 activation in AoSMCs from MEKK1^{-/-} mice was less than that from WT mice (Figure 3A). We confirmed that addition of MEKK1 restored MEKK1 protein levels in MEKK1^{-/-} AoSMCs (Figure 3B). Addition of MEKK1 restored JNK and ERK activation in response to FGF-2 in MEKK1^{-/-} AoSMCs (Figure 3C and 3D). Treatment with EGF or PDGF-BB instead of FGF-2 yielded identical results (data not shown).

MEKK1 Ablation Inhibited AoSMC Migration and Invasion

In the scrape wound-induced migration assays, the average number of and distance that MEKK1^{-/-} AoSMCs migrated

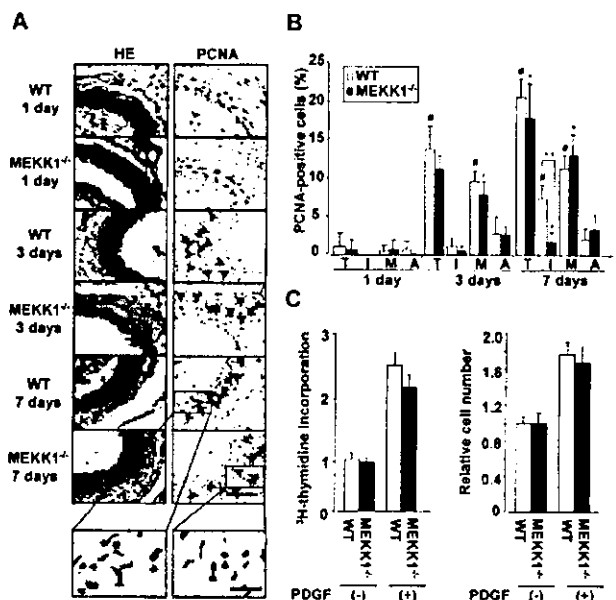


Figure 2. Effects of ablation of MEKK1 on cell proliferation. **A**, Immunohistochemical analysis of hematoxylin and eosin staining and PCNA staining 1, 3, and 7 days after ligation. Bar indicates 100 μm . Photographs of WT and MEKK1^{-/-} mice 7 days after ligation were enlarged, and bar indicates 30 μm . Red arrowheads indicate PCNA-positive cells. **B**, Quantification of ratio of PCNA-positive cells to total cell number in arterial wall (T), intima (I), media (M), and adventitia (A) of ligated arteries at 1, 3, and 7 days. Black bars and white bars indicate WT and MEKK1^{-/-} mice, respectively. # $P < 0.05$ vs day 1 in WT mice; * $P < 0.05$ vs day 1 in MEKK1^{-/-} mice; ** $P < 0.05$ vs day 7 in WT mice. **C**, Effects of MEKK1 on PDGF-BB-induced [³H]thymidine incorporation and cell number in AoSMCs. Data are indicated as percentages relative to control group and are mean \pm SEM of 10 wells in each group of at least 3 replicates.

from the wound edge (white dotted line) in the absence of any stimulus was similar to those in WT mice; however, the FGF-2-induced increase in cell number and distance was significantly suppressed in MEKK1^{-/-} AoSMCs compared with WT cells. Addition of MEKK1 restored the number and distance of MEKK1^{-/-} AoSMCs to normal levels (Figure 4A and 4B).

In the aortic explant assays, the number of AoSMCs migrating from MEKK1^{-/-} explants at 10 days was considerably lower than those from WT explants (Figure 4C). Moreover, the number of MEKK1^{-/-} aortic explants that showed migrating cells was significantly smaller than in WT explants (27.2 \pm 2.2% versus 60.0 \pm 2.5%, $P < 0.05$).

In the transwell Matrigel-coated chamber invasion assays, the number of invading MEKK1^{-/-} AoSMCs in response to FGF-2 was suppressed markedly compared with WT cells. Addition of MEKK1 restored the number of MEKK1^{-/-} AoSMCs to normal levels (Figure 4D). Treatment with EGF or PDGF-BB instead of FGF-2 yielded identical results (data not shown).

MEKK1 Ablation Impaired Lamellipodia Formation

There were no morphological differences between WT and MEKK1^{-/-} AoSMCs under basal conditions; however, typi-

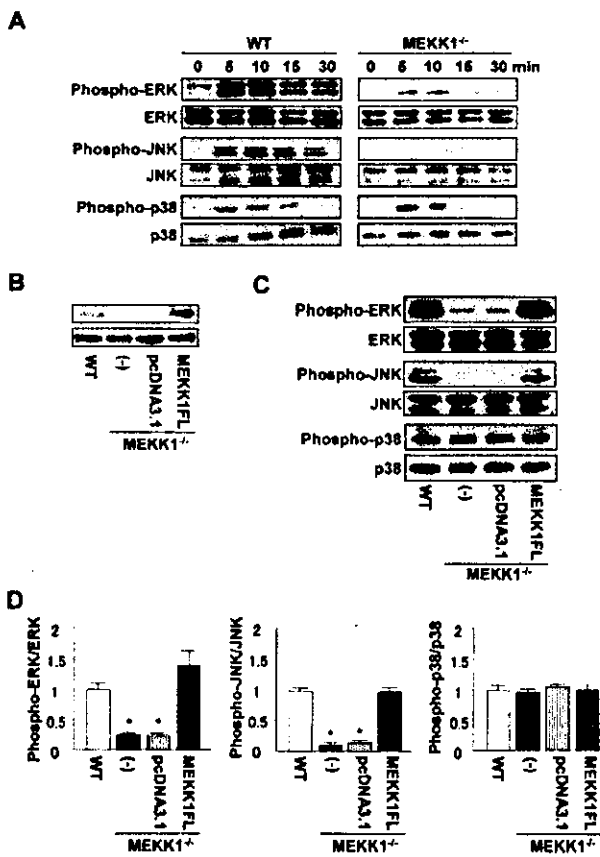


Figure 3. Effects of ablation of MEKK1 on MAPK activities in AoSMCs. **A**, Time course of JNK, ERK, and p38 activities followed by FGF-2 stimulation. **B**, Addition of MEKK1 experiments in MEKK1^{-/-} AoSMCs. **C**, Western blot analysis of MAPKs in MEKK1^{-/-} AoSMCs transfected with empty vector (pcDNA3.1) or full-length forms of MEKK1 vector (MEKK1FL) followed by FGF-2 stimulation. **D**, Cumulative data for MAPK in Figure 3C. **P*<0.05 vs WT AoSMCs.

cal lamellipodia formation was induced by treatment with EGF in WT AoSMCs but was seldom induced in MEKK1^{-/-} AoSMCs (Figure 5A). The percentage of MEKK1^{-/-} AoSMCs showing lamellipodia was significantly lower than in WT AoSMCs (*P*<0.05). Addition of MEKK1 restored the lamellipodia-forming capacity of MEKK1^{-/-} AoSMCs (Figure 5B). Treatment with FGF-2 or PDGF-BB instead of EGF yielded identical results (data not shown).

MEKK1 Ablation Decreased uPA Expression

uPA expression began to increase on day 1 and reached a peak on day 3, after which it decreased gradually by 7 days after ligation in WT mice. In contrast, there was only weak positive staining for uPA up to 7 days in MEKK1^{-/-} mice (Figure 6A). In vitro immunofluorescence staining revealed that PDGF-BB-induced uPA expression was decreased in MEKK1^{-/-} AoSMCs compared with those of WT mice (Figure 6B). Western blotting showed a dramatic reduction of FGF-2-induced uPA expression in MEKK1^{-/-} AoSMCs, which was restored by addition of MEKK1 (Figure 6C).

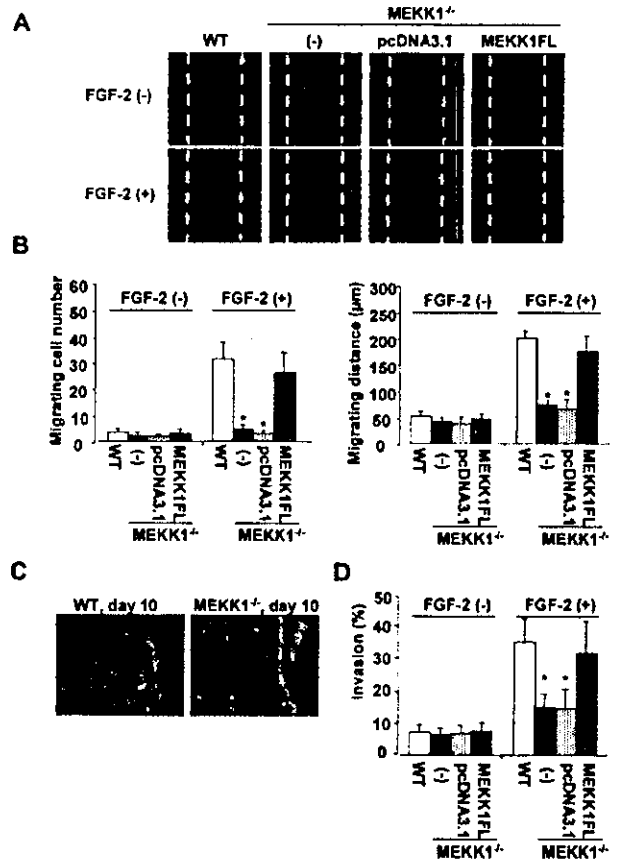


Figure 4. Migration and invasion of AoSMCs. **A**, Scrape wound-induced migration assay. Immunofluorescence microscopy of migrating cells from wound edge when AoSMCs were cultured for 24 hours with or without FGF-2. F-actin was stained with rhodamine-phalloidin (red), and nuclei were counterstained with DAPI (blue; not visible). **B**, Quantification of means of number and distance of migrating cells. **P*<0.05 vs WT AoSMCs. **C**, Migration of AoSMCs from aortic explants on day 10. **D**, Quantification of percent invasion of AoSMCs by transwell Matrigel-coated chamber invasion assay. **P*<0.05 vs WT AoSMCs.

Discussion

Several lines of evidence suggest that MEKK1 is implicated in diverse biological responses.⁶⁻⁸ Recently, the unique role of MEKK1 in regulating the migration of several cell types has aroused widespread attention^{9,12,27} and inspired us to study its involvement in cardiovascular diseases. Up to now, there has been no previous report on the role of MEKK1 in the development of vascular remodeling, during which invasion and proliferation of SMCs play key roles. In the present study, we investigated the mechanism whereby MEKK1 regulates vascular remodeling in a well-established, blood-flow cessation model in MEKK1^{-/-} mice. We found that MEKK1 is essential for intimal hyperplasia after cessation of blood flow.

In this study, we clearly demonstrated that intimal areas, I-M ratios, and stenotic ratios of the ligated arteries were significantly lower in MEKK1^{-/-} mice relative to WT mice, indicating that MEKK1 is implicated in intimal hyperplasia. Although an angioplasty/balloon injury model would have yielded greater applicability to the clinical situation, we used

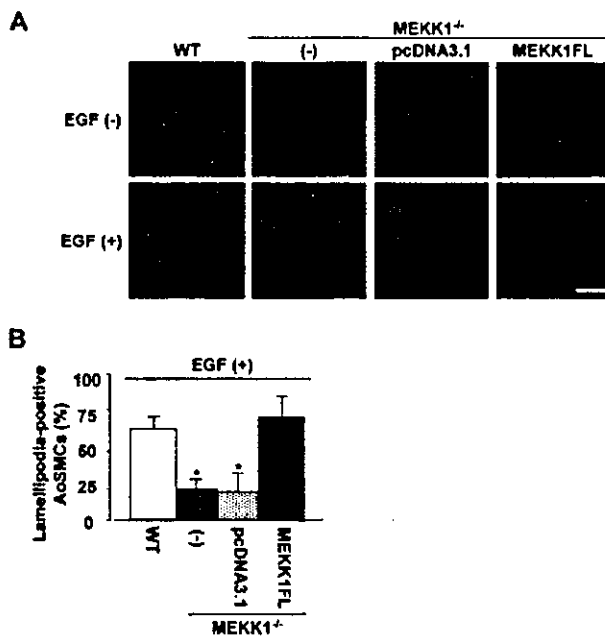


Figure 5. Lamellipodia formation in AoSMCs. A, Representative photomicrographs of lamellipodia formation in AoSMCs with or without EGF stimulation. Bar indicates 25 μ m. B, Percentage of lamellipodia-positive cells (n=100) in AoSMCs with EGF. *P<0.05 vs WT AoSMCs.

the ligation model because of its excellent reproducibility. To clarify the mechanism(s) of MEKK1 involvement, we first examined cell proliferation within the arterial wall after ligation and found no statistically significant difference in the

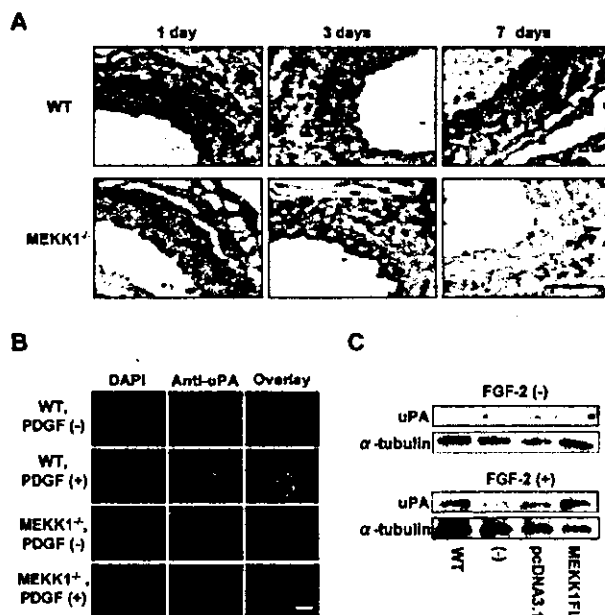


Figure 6. Expression of uPA in AoSMCs. A, Immunohistochemical analysis of time course of uPA expression 1, 3, and 7 days after ligation of carotid arteries. Bar indicates 100 μ m. B, Immunofluorescence staining for uPA in AoSMCs stimulated with PDGF-BB. Bar indicates 10 μ m. C, Western blots of uPA in AoSMCs stimulated with FGF-2.

number of PCNA-positive cells between WT and MEKK1^{-/-} mice. Results from this ligation model are consistent with the fact that MEKK1^{-/-} mice have no overt defects in growth and fertility.⁹ There was also no difference in the proliferation of WT and MEKK1^{-/-} AoSMCs evaluated by [³H]thymidine incorporation and cell number. These findings suggest that SMC proliferation might not contribute to the reduced intimal hyperplasia in MEKK1^{-/-} mice. Then we investigated SMC migration and uPA expression, both of which are important factors for intimal hyperplasia.

We demonstrated that there were significantly fewer intimal PCNA-positive cells 7 days after ligation in MEKK1^{-/-} mice than in WT mice. Because PCNA-positive cells are believed to migrate from the media to the intima,² this finding suggests that SMC migration is impaired in MEKK1^{-/-} mice. To directly assess the effects of MEKK1 ablation on SMC migration, we used several migration and invasion assays in vitro. We observed comparable migration or invasion of SMCs under control condition between WT and MEKK1^{-/-} AoSMCs; however, significant impairment of migration or invasion was observed after stimulation with FGF-2 in MEKK1^{-/-} AoSMCs, which was restored by addition of full-length MEKK1. These findings indicate that ablation of MEKK1 impairs invasion and migration, both of which may contribute to reduced intimal hyperplasia wherein growth factors may play a vital role.

Lamellipodia formation is essential for cell migration.¹³ Exogenous stimuli, such as PDGF or FGF-2, induce lamellipodia formation that can help to complete the first step of the motility cycle.^{14,28} Therefore, we examined whether MEKK1 is involved in lamellipodia formation in AoSMCs. Our results showed that the percentage of lamellipodia-positive cells was significantly smaller in MEKK1^{-/-} AoSMCs compared with WT AoSMCs in the presence of EGF. This finding suggests that the impairment of migration in MEKK1^{-/-} AoSMCs may be due to inhibited formation of lamellipodia. Indeed, addition of MEKK1 to MEKK1^{-/-} AoSMCs recovered their capacity to form lamellipodia and migrate. On the other hand, it has been reported that loss of MEKK1 disrupts focal adhesion composition, with decreased vinculin content and focal adhesion kinase (FAK) cleavage.²⁹ Because disruption of focal adhesion composition will affect cell migration, further investigation will be needed to clarify its role in MEKK1^{-/-} mice.

There is evidence that uPA is induced after arterial injury.^{5,28,30,31} uPA enhances vascular remodeling by transforming plasminogen into plasmin, which can activate metalloproteinases and in turn degrade ECM proteins.^{5,30,31} We found that uPA expression began to increase at 1 day and reached a peak 3 days after ligation in WT mice, whereas uPA staining appeared to be significantly lower in MEKK1^{-/-} arteries at corresponding times. In vitro, PDGF-BB- and FGF-2-induced uPA expression as detected by immunofluorescence staining and Western blotting was also significantly decreased in MEKK1^{-/-} AoSMCs. Thus, in addition to impaired lamellipodia formation, inhibited uPA expression by MEKK1 ablation may also contribute to impairment of SMC invasion. Addition of full-length MEKK1 restored uPA expression in MEKK1^{-/-} AoSMCs.

Although it has been reported that MEKK1 is required for FGF-2-induced signals to control uPA expression in fibroblasts,¹⁵ further investigations will be needed to elucidate the mechanism by which MEKK1 regulates uPA expression in arteries after ligation.

Recent studies have demonstrated that JNK and ERK transduction pathways may regulate cell migration^{32,33} and uPA expression.^{34,35} In the present study, we demonstrated that JNK and ERK activation after growth factor stimulation was blunted in MEKK1^{-/-} AoSMCs. Thus, it is possible that ablation of MEKK1 may inhibit cell migration and uPA expression by interfering with the downstream signaling pathways JNK and/or ERK. MEKK1 also has been reported to be associated with cytoskeletal reorganization^{11,12} and to be necessary for uPA upregulation,¹⁵ suggesting another possibility that ablation of MEKK1 directly inhibits lamellipodia formation and uPA expression. The stimulus for remodeling after ligation is also influenced by the resultant vascular ischemia. Because MEKK1 is activated by hypoxic stimuli as well as growth factors,³⁶ we must consider the possibility that the resultant hypoxic stimuli are also important during vascular remodeling in the ligation model.

Izumi et al²² demonstrated that activation of apoptosis signal-regulating kinase 1 (ASK1), another member of the MAP3K family, also plays a key role during intimal hyperplasia in the carotid artery balloon injury model. Unlike MEKK1, ablation of ASK1 blunted both JNK and p38 but not ERK activation in AoSMCs after serum stimulation. In addition, ablation of ASK1 caused impairment of both SMC migration and proliferation. Thus, although the methods or models used to evaluate functions of MEKK1 and ASK1 were not the same, both MEKK1 and ASK1 may contribute to the development of intimal hyperplasia by different mechanisms.

In conclusion, we have demonstrated that MEKK1 plays a critical role during intimal hyperplasia in a mouse carotid blood-flow cessation model. Intimal hyperplasia is greatly lessened, possibly due to a reduction of SMC invasion by an impairment of their migration and reduced uPA expression. We propose that MEKK1 is a potential target for drug development to prevent vascular remodeling.

Acknowledgments

This study was supported by grants on Human Genome, Tissue Engineering, and Food Biotechnology (H13-genome-11) and grants on Comprehensive Research on Aging and Health [H13-21seiki(seikatsu)-23] in Health and Labor Science Research from the Ministry of Health, Labor, and Welfare, Japan. We thank Hiroko Okuda for technical assistance and Yukari Arino for secretarial work.

References

- Sakaguchi T, Yan SF, Yan SD, Belov D, Rong LL, Sousa M, Andrassy M, Marso SP, Duda S, Arnold B, Liliensiek B, Nawroth PP, Stern DM, Schmidt AM, Naka Y. Central role of RAGE-dependent neointimal expansion in arterial restenosis. *J Clin Invest*. 2003;111:959-972.
- Newby AC, Zaltsman AB. Molecular mechanisms in intimal hyperplasia. *J Pathol*. 2000;190:300-309.
- Maheshwari G, Lauffenburger DA. Deconstructing (and reconstructing) cell migration. *Microsc Res Tech*. 1998;43:358-368.
- Reidy MA, Irvin C, Lindner V. Migration of arterial wall cells: expression of plasminogen activators and inhibitors in injured rat arteries. *Circ Res*. 1996;78:405-414.
- Carmeliet P, Moons L, Herbert JM, Crawley J, Lijnen R, Collen D. Urokinase but not tissue plasminogen activator mediates arterial neointima formation in mice. *Circ Res*. 1997;81:829-839.
- Minamino T, Yujiri T, Terada N, Taffet GE, Michael LH, Johnson GL, Schneider MD. MEKK1 is essential for cardiac hypertrophy and dysfunction induced by Gq. *Proc Natl Acad Sci U S A*. 2002;99:3866-3871.
- Yujiri T, Sather S, Fanger GR, Johnson GL. Role of MEKK1 in cell survival and activation of JNK and ERK pathways defined by targeted gene disruption. *Science*. 1998;282:1911-1914.
- Minamino T, Yujiri T, Papst PJ, Chan ED, Johnson GL, Terada N. MEKK1 suppresses oxidative stress-induced apoptosis of embryonic stem cell-derived cardiac myocytes. *Proc Natl Acad Sci U S A*. 1999;96:15127-15132.
- Yujiri T, Ware M, Widmann C, Oyer R, Russell D, Chan E, Zaitis Y, Clarke P, Tyler K, Oka Y, Fanger GR, Henson P, Johnson GL. MEK kinase 1 gene disruption alters cell migration and c-Jun NH₂-terminal kinase regulation but does not cause a measurable defect in NF- κ B activation. *Proc Natl Acad Sci U S A*. 2000;97:7272-7277.
- Xia Y, Makris C, Su B, Li E, Yang J, Nemerow GR, Karin M. MEK kinase 1 is critically required for c-Jun N-terminal kinase activation by proinflammatory stimuli and growth factor-induced cell migration. *Proc Natl Acad Sci U S A*. 2000;97:5243-5248.
- Christerson LB, Vanderbilt CA, Cobb MH. MEKK1 interacts with α -actinin and localizes to stress fibers and focal adhesions. *Cell Motil Cytoskeleton*. 1999;43:186-198.
- Yujiri T, Fanger GR, Garrington TP, Schlesinger TK, Gibson S, Johnson GL. MEK kinase 1 (MEKK1) transduces c-Jun NH₂-terminal kinase activation in response to changes in the microtubule cytoskeleton. *J Biol Chem*. 1999;274:12605-12610.
- Small JV, Stradal T, Vignal E, Rottner K. The lamellipodium: where motility begins. *Trends Cell Biol*. 2002;12:112-120.
- DesMarais V, Ichetovkin I, Condeelis J, Hitchcock-DeGregori SE. Spatial regulation of actin dynamics: a tropomyosin-free, actin-rich compartment at the leading edge. *J Cell Sci*. 2002;115:4649-4660.
- Witowsky J, Abell A, Johnson NL, Johnson GL, Cuevas BD. MEKK1 is required for inducible urokinase-type plasminogen activator expression. *J Biol Chem*. 2003;278:5941-5946.
- Kumar A, Lindner V. Remodeling with neointima formation in the mouse carotid artery after cessation of blood flow. *Arterioscler Thromb Vasc Biol*. 1997;17:2238-2244.
- Schafer K, Konstantinides S, Riedel C, Thinnis T, Muller K, Dellas C, Hasenfuss G, Loskutoff DJ. Different mechanisms of increased luminal stenosis after arterial injury in mice deficient for urokinase- or tissue-type plasminogen activator. *Circulation*. 2002;106:1847-1852.
- Murakoshi N, Miyauchi T, Kakinuma Y, Ohuchi T, Goto K, Yanagisawa M, Yamaguchi I. Vascular endothelin-B receptor system in vivo plays a favorable inhibitory role in vascular remodeling after injury revealed by endothelin-B receptor-knockout mice. *Circulation*. 2002;106:1991-1998.
- Kuzuya M, Kanda S, Sasaki T, Tamaya-Mori N, Cheng XW, Itoh T, Itoharu S, Iguchi A. Deficiency of gelatinase A suppresses smooth muscle cell invasion and development of experimental intimal hyperplasia. *Circulation*. 2003;108:1375-1381.
- Bradshaw AD, Francki A, Motamed K, Howe C, Sage EH. Primary mesenchymal cells isolated from SPARC-null mice exhibit altered morphology and rates of proliferation. *Mol Biol Cell*. 1999;10:1569-1579.
- Yujiri T, Nawata R, Takahashi T, Sato Y, Tanizawa Y, Kitamura T, Oka Y. MEK kinase 1 interacts with focal adhesion kinase and regulates insulin receptor substrate-1 expression. *J Biol Chem*. 2003;278:3846-3851.
- Izumi Y, Kim S, Yoshiyama M, Izumiya Y, Yoshida K, Matsuzawa A, Koyama H, Nishizawa Y, Ichijo H, Yoshikawa J, Iwao H. Activation of apoptosis signal-regulating kinase 1 in injured artery and its critical role in neointimal hyperplasia. *Circulation*. 2003;108:2812-2818.
- Galis ZS, Johnson C, Godin D, Magid R, Shipley JM, Senior RM, Ivan E. Targeted disruption of the matrix metalloproteinase-9 gene impairs smooth muscle cell migration and geometrical arterial remodeling. *Circ Res*. 2002;91:852-859.
- Hsieh CC, Lau Y. Migration of vascular smooth muscle cells is enhanced in cultures derived from spontaneously hypertensive rat. *Pflugers Arch*. 1998;435:286-292.

25. Chaulet H, Desgranges C, Renault MA, Dupuch F, Ezan G, Peiretti F, Loirand G, Pacaud P, Gadeau AP. Extracellular nucleotides induce arterial smooth muscle cell migration via osteopontin. *Circ Res*. 2001;89:772-778.
26. Watanabe M, Yano W, Kondo S, Hattori Y, Yamada N, Yanai R, Nishida T. Up-regulation of urokinase-type plasminogen activator in corneal epithelial cells induced by wounding. *Invest Ophthalmol Vis Sci*. 2003;44:3332-3338.
27. Zhang L, Deng M, Kao CW, Kao WW, Xia Y. MEK kinase 1 regulates c-Jun phosphorylation in the control of corneal morphogenesis. *Mol Vis*. 2003;9:584-593.
28. Kessels MM, Engqvist-Goldstein AE, Drubin DG. Association of mouse actin-binding protein 1 (mAbp1/SH3P7), an Src kinase target, with dynamic regions of the cortical actin cytoskeleton in response to Rac1 activation. *Mol Biol Cell*. 2000;11:393-412.
29. Cuevas BD, Abell AN, Witowsky JA, Yujiri T, Johnson NL, Kesavan K, Ware M, Jones PL, Weed SA, DeBiasi RL, Oka Y, Tyler KL, Johnson GL. MEKK1 regulates calpain-dependent proteolysis of focal adhesion proteins for rear-end detachment of migrating fibroblasts. *EMBO J*. 2003;22:3346-3355.
30. Carmeliet P, Moons L, Lijnen R, Baes M, Lemaitre V, Tipping P, Drew A, Eeckhout Y, Shapiro S, Lupu F, Collen D. Urokinase-generated plasmin activates matrix metalloproteinases during aneurysm formation. *Nat Genet*. 1997;17:439-444.
31. Lamfers ML, Lardenoye JH, de Vries MR, Aalders MC, Engelse MA, Grimbergen JM, van Hinsbergh VW, Quax PH. In vivo suppression of restenosis in balloon-injured rat carotid artery by adenovirus-mediated gene transfer of the cell surface-directed plasmin inhibitor ATF.BPTI. *Gene Ther*. 2001;8:534-541.
32. Xia Y, Karin M. The control of cell motility and epithelial morphogenesis by Jun kinases. *Trends Cell Biol*. 2004;14:94-101.
33. Matsubayashi Y, Ebisuya M, Honjoh S, Nishida E. ERK activation propagates in epithelial cell sheets and regulates their migration during wound healing. *Curr Biol*. 2004;14:731-735.
34. Benasciutti E, Pages G, Kenzior O, Folk W, Blasi F, Crippa MP. MAPK and JNK transduction pathways can phosphorylate Sp1 to activate the uPA minimal promoter element and endogenous gene transcription. *Blood*. 2004;104:256-262.
35. Jo M, Thomas KS, O'Donnell DM, Gonias SL. Epidermal growth factor receptor-dependent and -independent cell-signaling pathways originating from the urokinase receptor. *J Biol Chem*. 2003;278:1642-1646.
36. Lee SR, Lo EH. Interactions between p38 mitogen-activated protein kinase and caspase-3 in cerebral endothelial cell death after hypoxia-reoxygenation. *Stroke*. 2003;34:2704-2709.

Benidipine, a long-acting calcium channel blocker, inhibits cardiac remodeling in pressure-overloaded mice

Yulin Liao^a, Masanori Asakura^a, Seiji Takashima^a, Akiko Ogai^b, Yoshihiro Asano^a,
Hiroshi Asanuma^a, Tetsuo Minamino^a, Hitonobu Tomoike^b,
Masatsugu Hori^a, Masafumi Kitakaze^{b,*}

^aDepartment of Internal Medicine and Therapeutics, Osaka University Graduate School of Medicine, 2-2 Yamadaoka, Suita, Osaka 565-0781, Japan

^bCardiovascular Division of Internal Medicine, National Cardiovascular Center (M.K.), 5-7-1 Fujishirodai, Suita, Osaka 565-8565, Japan

Received 9 August 2004; received in revised form 25 October 2004; accepted 3 November 2004

Available online 24 November 2004

Time for primary review 19 days

Abstract

Objective: The effects of long-acting calcium channel blockers (CCBs) on pressure overload-induced cardiac remodeling are seldom studied in animals. We evaluated the effects of benidipine, a long-acting CCB, on cardiac remodeling.

Methods: Rat neonatal cardiac myocytes were used to examine the influence of benidipine on protein synthesis. Cardiac remodeling was induced in C57 B6/J mice by transverse aortic constriction (TAC). Then the effects of benidipine (10 mg/kg/d) were assessed on myocardial hypertrophy and heart failure, cardiac histology, and gene expression.

Results: Benidipine significantly inhibited protein synthesis by cardiac myocytes stimulated with phenylephrine (PE), and this effect was partially abolished by cotreatment with a nitric oxide synthase (NOS) inhibitor [N(G)-nitro-L-arginine methylester (L-NAME)]. Four weeks after the onset of pressure overload, benidipine therapy potently inhibited cardiac hypertrophy and prevented heart failure. The heart to body weight ratio was 6.89 ± 0.48 mg/g in treated mice vs. 8.76 ± 0.33 mg/g in untreated mice ($P < 0.01$), and the lung to body weight ratio was 7.39 ± 0.93 mg/g vs. 10.53 ± 0.99 mg/g, respectively ($P < 0.05$). Left ventricular fractional shortening (LVFS) was improved on echocardiography. Plasma NO levels were increased, while B type natriuretic peptide, protein inhibitor of neuronal NOS, and procollagen IV alpha were down-regulated in benidipine-treated mice.

Conclusion: These results indicate that benidipine inhibits cardiac remodeling due to pressure overload at least partly by acting on the nitric oxide signaling pathway.

© 2004 European Society of Cardiology. Published by Elsevier B.V. All rights reserved.

Keywords: Calcium channel blocker; Heart failure; Hypertrophy; Gene expression

1. Introduction

Calcium channel blockers (CCBs) are one of the most frequently used classes of drugs for the treatment of hypertension. Although early clinical studies showed a disappointing outcome when short-acting dihydropyridine CCBs were used to reduce cardiovascular risk [1,2], well-designed prospective randomized controlled clinical trials have dem-

onstrated that long-acting dihydropyridine CCBs are effective for reduction of the blood pressure (BP), inhibition of cardiac remodeling, and decreasing the risk of cardiovascular endpoints [3]. However, the underlying mechanism of the beneficial effect of CCBs on cardiac remodeling is not fully understood. An earlier study performed by our laboratory showed that the vasodilator hydralazine significantly lowered the systemic blood pressure but did not exert any effect on cardiac hypertrophy induced in rats by N(G)-nitro-L-arginine methylester (L-NAME), a nitric oxide (NO) synthase inhibitor [4], suggesting that blood pressure reduction alone was not sufficient to inhibit cardiac remodeling. We also

* Corresponding author. Tel.: +81 6 6833 5012x2225; fax: +81 6 6836 1120.

E-mail address: kitakazc@zf6.so-net.ne.jp (M. Kitakaze).

reported that a long-acting CCB, benidipine, could increase coronary flow and reduce myocardial ischemia by promoting the release of NO [5,6]. NO is also known to lessen the severity of cardiac hypertrophy and heart failure [7,8]. Furthermore, benidipine has been demonstrated to inhibit myocardial fibrosis in diabetic rats [9]. Based on these lines of evidence, we hypothesized that benidipine may inhibit cardiac remodeling via the NO signaling pathway.

Because the occurrence of cardiac remodeling has been shown to be associated with subsequent cardiovascular events, therapeutic approaches that inhibit cardiac remodeling are likely to improve the prognosis. Chronic left ventricular pressure overload induced by transverse aortic constriction (TAC) is a well established animal model for investigation of cardiac remodeling [10–12], but few experimental studies have attempted to clarify the effects of long-acting CCBs on cardiac remodeling using this model. Therefore, we evaluated the effects of benidipine on cardiac hypertrophy and heart failure in a murine model of pressure overload due to TAC and explored the mechanisms involved.

2. Methods

2.1. Cell culture

Rat neonatal cardiac myocytes were isolated, as described previously [13]. The myocytes were cultured in Dulbecco's modified Eagle's medium (DMEM; Sigma) supplemented with 10% FBS (Equitech-Bio), which was changed to serum-free medium after 72 h. Cells were cultured under serum-free conditions for 48 h before agents were added. Protein synthesis by cultured cells was evaluated from [³H] leucine incorporation, as described elsewhere [11,13]. Cardiac myocytes were exposed to 10⁻⁴ M phenylephrine (PE) for 24 h in the presence or absence of benidipine (kindly provided by the Pharmaceutical Research Laboratories of Kyowa Hakko Kogyo Sunto, Shizuoka, Japan), and the increase of [³H] leucine uptake was examined. To determine whether the NO signaling pathway was involved in the inhibition of protein synthesis by cardiac myocytes, we examined whether the *in vitro* effect of benidipine could be blocked by the NO synthase (NOS) inhibitor L-NAME (10⁻⁵ M).

2.2. Animal model

All procedures were performed in accordance with the Guide for the Care and Use of Laboratory Animals published by the US National Institutes of Health (NIH Publication No. 85–23, revised 1996). Male C57BL/6J mice aged 8–9 weeks and weighing 19–23 g were anesthetized with a mixture of xylazine (5 mg/kg) and ketamine (100 mg/kg) injected intraperitoneally. Then pressure overload was created, as described previously [10]. Briefly, endotracheal intubation was performed, and the cannula was connected to

a volume-cycled rodent ventilator with a tidal volume of 0.5 ml (room air) and a respiration rate of 100/min. The chest was entered via the second intercostal space at the upper left sternal border. After the arch of the aorta was isolated, TAC was created using a 7–0 suture tied twice around a 27-gauge needle and the aortic arch between the innominate and left common carotid arteries. After the suture was tied, the needle was gently removed, yielding 60–80% constriction of the aorta. More than 1000 murine TAC models have been created at our laboratory, and cardiac hypertrophy occurs in 100% of these animals. The dispersion of heart weight to body weight ratio evaluated with statistical parameter coefficient variance at 4 weeks following TAC is about 20%, as we reported previously [11,14].

To test whether benidipine could inhibit the cardiac hypertrophy due to TAC, we treated the mice with either saline (TAC group) or benidipine at 10 mg/kg/d (po, mixed with 0.3% carboxymethyl cellulose sodium and suspended in water) from the 2nd day after surgery. The benidipine dose was based on previous reports from our [4] and another [9] laboratory as well as a preliminary study. To confirm that the extent of the pressure overload was similar between benidipine-treated and untreated animals, three mice were randomly selected from each group to measure the pressure in ascending aorta, using a 1.4 F Millar Pressure Catheter on the 2nd day after TAC. Four weeks after the creation of pressure overload, both the tail cuff blood pressure (BP) and the heart rate (HR; BP-98A, Softron, Tokyo, Japan) were measured 1 day before sacrifice. LV hemodynamic studies were performed by cannulation of the right carotid artery with a Millar Pressure Catheter that was carefully advanced to the LV. Then the mice were killed to measure organ weights and to perform histological analysis.

2.3. Histological examination

The cross-sectional area of cardiac myocytes and the extent of myocardial fibrosis were measured, as described elsewhere [4,15]. Briefly, the cardiac myocyte area and myocardial fibrosis area were analyzed quantitatively by morphometry of either HE-stained or Azan/Mallory-stained sections. The original images were digitized and transformed into binary images, after which the cardiac myocyte area or fibrosis area was calculated with an automatic area quantification program (NIH Image). One hundred myocytes per heart were counted, and the average value was determined. The total myocardial fibrosis index was defined as the sum of the total area of fibrosis in the entire microscopic field divided by the sum of total connective tissue area plus the myocardial area in the entire field.

2.4. Echocardiography

Transthoracic echocardiography was performed with a Sonos 4500 and a 15–6 L MHz transducer (Philips, the Netherlands). Mice were weighed, lightly anesthetized with

2.5% avertin (0.06 ml/10 g), and set in the left lateral decubitus position or the supine position. After the mouse recovered to complete consciousness (about 10 min), two-dimensional short-axis views of the left ventricle were obtained for guided M-mode measurement of the left ventricular diastolic posterior wall thickness (LVPWd), left ventricular end-diastolic dimension (LVEDd), and left ventricular end-systolic dimension (LVESd). Left ventricular fractional shortening (LVFS) was calculated as follows: $LVFS = (LVEDd - LVESd) / LVEDd * 100$.

2.5. Microarray analysis

To determine the gene expression profile during cardiac remodeling, we performed microarray studies of murine hearts after pressure overload for 1 or 4 weeks. Data about the time course of the induction of NO synthase and fibrosis-related genes were needed to investigate their roles in cardiac hypertrophy and heart failure. Total RNA was prepared from murine hearts using Triazol (Gibco-BRL), according to the manufacturer's instructions. Microarray hybridization was performed in duplicate using Affymetrix Murine Genome U74v2A gene chips and RNA from hearts of animals in the TAC or sham operation groups at 1 or 4 weeks after surgery. Data were analyzed using Genespring 6 software [16].

2.6. Measurement of plasma nitric oxide

Blood was obtained from the right ventricle with a 23-gauge needle at the time of sacrificing the mice. The plasma concentrations of NOx (NO₂+NO₃) was measured with an autoanalyzer (ENO-10, Eicom Kyoto, Japan), as described elsewhere [5,6,17]. Samples were applied to an analytical column that was connected to a copperized cadmium reduction column to reduce NO₂ to NO₃, which was then reacted with Griess reagent, and the absorbance of the product was measured at 540 nm.

2.7. Quantitative PCR

Based on the results of microarray analysis, we chose three genes that were consistently up-regulated at both 1 and 4 weeks after the onset of LV pressure overload and were closely related to cardiac hypertrophy or heart failure. We further investigated the effects of benidipine on these genes by real-time PCR. The three genes were the natriuretic peptide precursor type B (BNP) gene, protein inhibitor of neuronal nitric oxide synthase (PIN) gene, and procollagen IV alpha gene. Primers were designed using Gene Express software. Using 50 ng/ μ l of total RNA as the template, quantitative measurement was performed with an ABI Prism 7700 sequencing system. Amplification was done by the one-step method using a Quantitect SYBR Green RT-PCR kit (QIAGEN). Glyceraldehyde-3-phosphate dehydrogenase (GAPDH) was amplified as an endogenous control, and quantitation of target gene levels was performed relative to this gene.

2.8. Statistical analysis

For all statistical tests, multiple comparison was performed by one-way ANOVA with the Tukey–Kramer exact probability test. The least-squares method was used for linear correlation between selected variables. Results are reported as the mean \pm S.E.M., and $P < 0.05$ was considered statistically significant.

3. Results

3.1. Benidipine reduces cardiac myocyte protein synthesis stimulated by PE

Benidipine (10^{-4} M) did not affect basal [³H] leucine uptake by cardiac myocytes, but it inhibited PE-induced

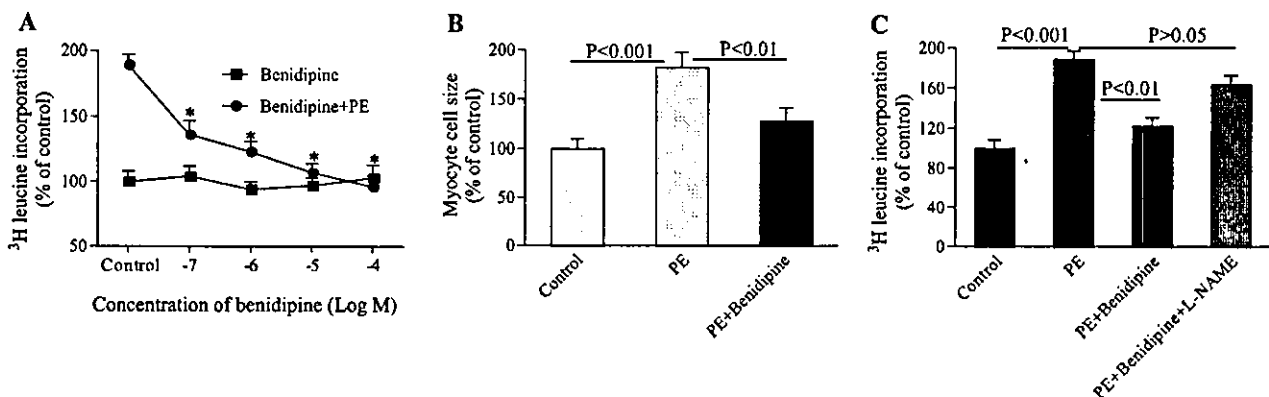


Fig. 1. Effect of benidipine on protein synthesis and the size of neonatal rat cardiac myocytes. (A) Protein synthesis stimulated by 10^{-4} M phenylephrine (PE) was inhibited by benidipine at concentrations ranging from 10^{-7} – 10^{-4} M in a dose-independent fashion, and this concentration range did not affect normal cardiac myocytes. * $P < 0.01$ vs. control. (B) The cell size was calculated from 200 cells in every group. The increase of cell size caused by PE (10^{-4} M) was inhibited by treatment with benidipine (10^{-5} M). (C) The inhibitory effect of benidipine (10^{-5} M) on protein synthesis induced by PE was partially blocked by cotreatment with L-NAME (10^{-5} M).

Table 1
Hemodynamic and echocardiographic data obtained at 4 weeks

Group	BW (g)	HR (bpm)	SBP (mm Hg)	LVPWd (mm)	LVEDd (mm)	LVESd (mm)
Sham	25.2±0.4**	651±11	114±3	0.65±0.02***	3.07±0.06	1.64±0.04**
TAC	22.64±0.41	686±26	101±5	0.98±0.04	3.38±0.12	2.29±0.04
TAC+Beni	23.1±0.4	652±26	105±2	0.77±0.03***	3.04±0.06*	1.69±0.12**

Beni—benidipine (10 mg/kg/d po); BW—body weight; HR—heart rate; SBP—Tail cuff systolic blood pressure; LVPWd—LV diastolic posterior wall thickness; LVEDd—LV end-diastolic dimension; LVESd—left ventricular end-systolic dimension. The number of mice in the sham, TAC, and TAC+benidipine groups was 10, 17, and 11, respectively, for BW, LVPWd, LVEDd, and LVESd; and 10, 9, and 7 for HR and SBP.

* $P < 0.05$.

** $P < 0.01$.

*** $P < 0.001$ vs. TAC (transverse aortic constriction).

protein synthesis in a concentration-dependent fashion (Fig. 1A). The enlargement of cells induced by PE was also inhibited by benidipine (Fig. 1B). The inhibitory effect of benidipine on PE-induced protein synthesis was partially blocked by L-NAME (Fig. 1C).

3.2. Benidipine inhibits pathological cardiac hypertrophy

The hemodynamic and echocardiographic data obtained just before sacrifice are shown in Table 1. Benidipine (10 mg/kg/d) did not significantly affect the tail cuff systolic blood pressure, but the LV wall was thinner, and LV dimensions were smaller in benidipine-treated mice than in TAC mice (Table 1).

Echocardiography and hemodynamics showed no differences among the three groups of mice before surgery (data not shown). The ascending aortic systolic blood pressure

was measured on the 2nd day after TAC or sham operation without drug treatment in order to evaluate the extent of pressure overload (in three mice per group), no significant difference was noted between the TAC and benidipine groups (98 ± 5 mm Hg in the sham group, 163 ± 4 mm Hg in the TAC group, and 161 ± 3 mm Hg in the benidipine group).

LV hemodynamics were similar between TAC mice with or without benidipine treatment (Fig. 2), suggesting that an oral dose of 10 mg/kg did not significantly affect LV function.

Consistent with the in vitro results, benidipine markedly inhibited cardiac hypertrophy at 4 weeks after TAC (Fig. 3). Histological examination showed that the extent of myocyte hypertrophy (Fig. 4A,B) was reduced and that myocardial fibrosis was less severe in benidipine-treated mice (Fig. 4C,D).

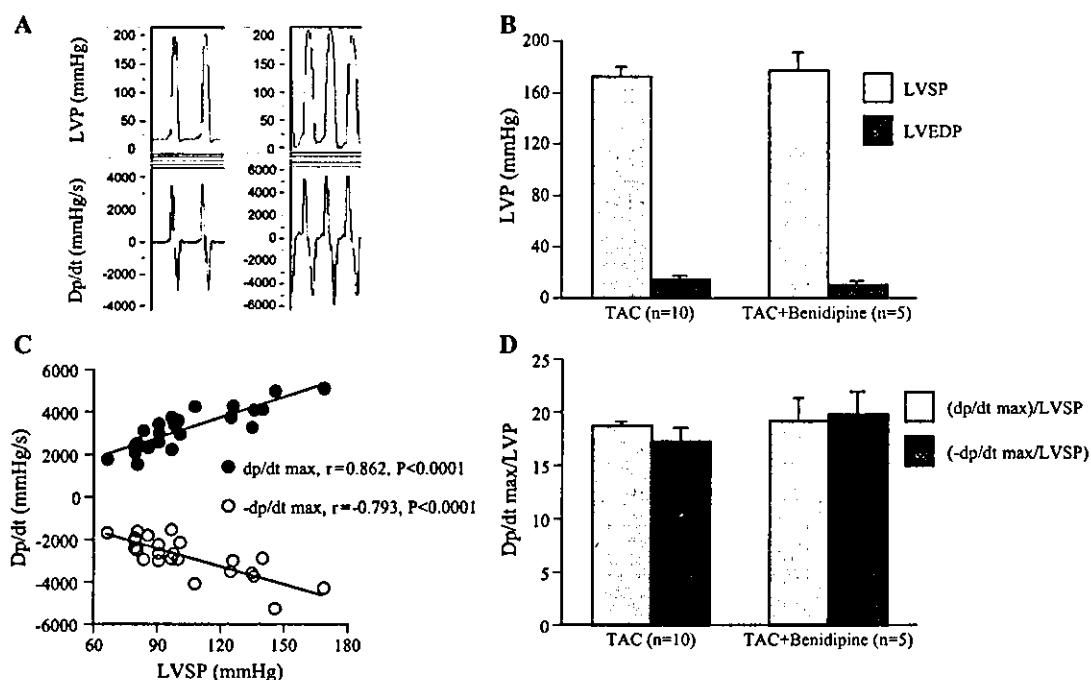


Fig. 2. Left ventricular (LV) hemodynamics measured with a Millar Catheter at 4 weeks after TAC. (A) LV pressure and dp/dt in the TAC and benidipine groups. (B) No significant differences of LV systolic pressure (LVSP) and LV end-diastolic pressure (LVEDP) were noted between TAC mice with or without benidipine. (C) \pm Dp/dt max was closely correlated with LVSP in untreated mice. (D) \pm Dp/dt max/LVSP was not significantly increased in benidipine-treated mice.